AD-A034 044 DAVID W TAYLOR NAVAL SHIP RESEARCH AND DEVELOPMENT CE--ETC F/G 20/4
ANALYSIS OF WAKE SURVEY DATA FOR A GUIDED MISSILE STRIKE CRUISE--ETC(U)
DEC 76 A C LIN, R B HURWITZ

UNCLASSIFIED SPD-724-05 NL

| OF |
AD
A034044

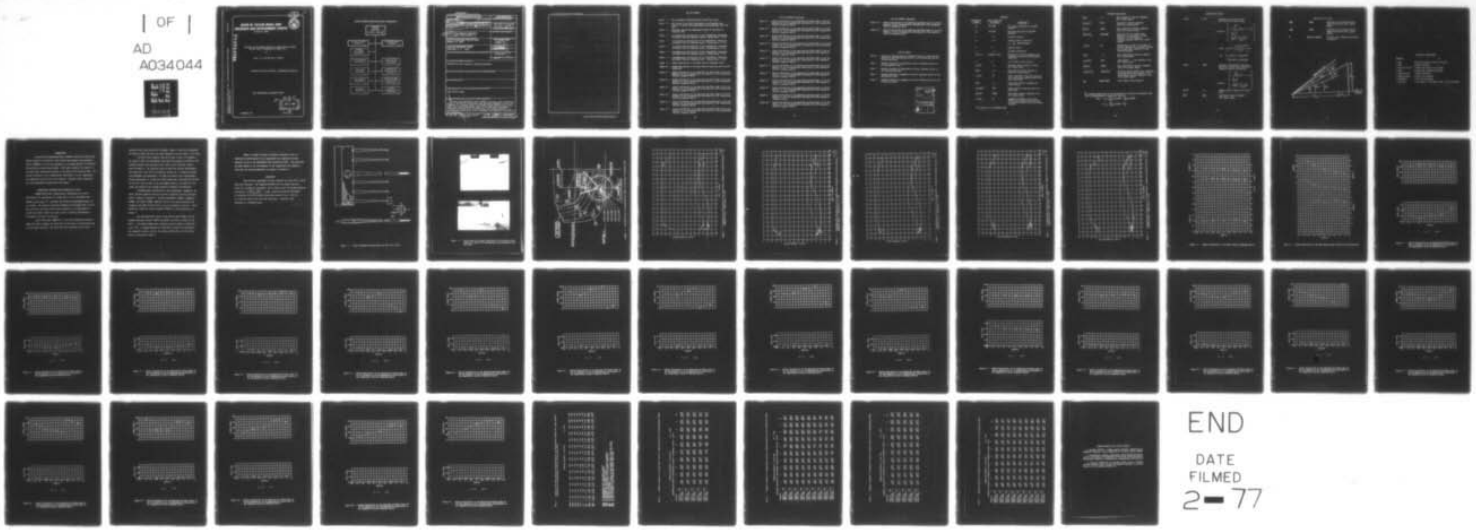

END

DATE
FILMED
2-77

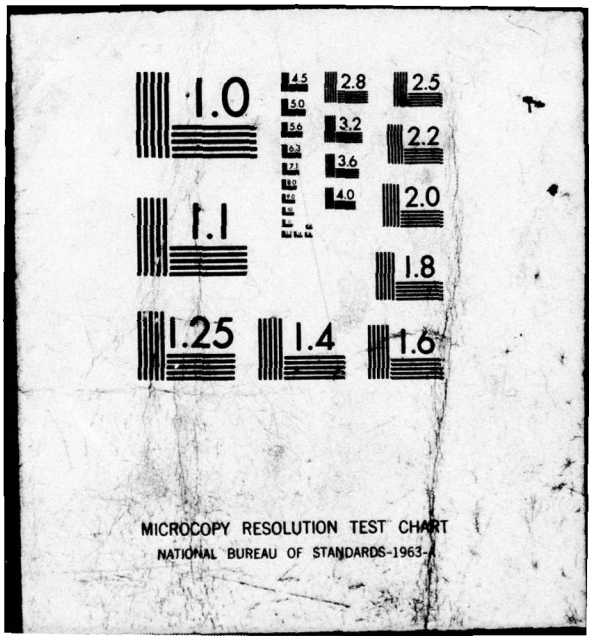
1.0
1.1
1.25
1.4
1.6
1.8
2.0
2.2
2.5
2.8
3.2
3.6
4.0
4.5
5.0
5.6
6.3
7.1
8.0
9.0
MICROCOPY RESOLUTION TEST CHART
NATIONAL BUREAU OF STANDARDS-1963-A

DAVID W. TAYLOR NAVAL SHIP RESEARCH AND DEVELOPMENT CENTER

Bethesda, Md. 20084

ANALYSIS OF WAKE SURVEY DATA FOR A GUIDED MISSILE STRIKE CRUISER (CSGN) REPRESENTED BY MODEL 5352

BY

ALAN C. M. LIN AND RAE B. HURWITZ

SHIP PERFORMANCE DEPARTMENT REPORT

DECEMBER 1976

SPD-724-05

SPD-724-05

ANALYSIS OF WAKE SURVEY DATA FOR A GUIDED MISSILE STRIKE CRUISER (CSGN) REPRESENTED BY MODEL 5352

MAJOR DTNSRDC ORGANIZATIONAL COMPONENTS

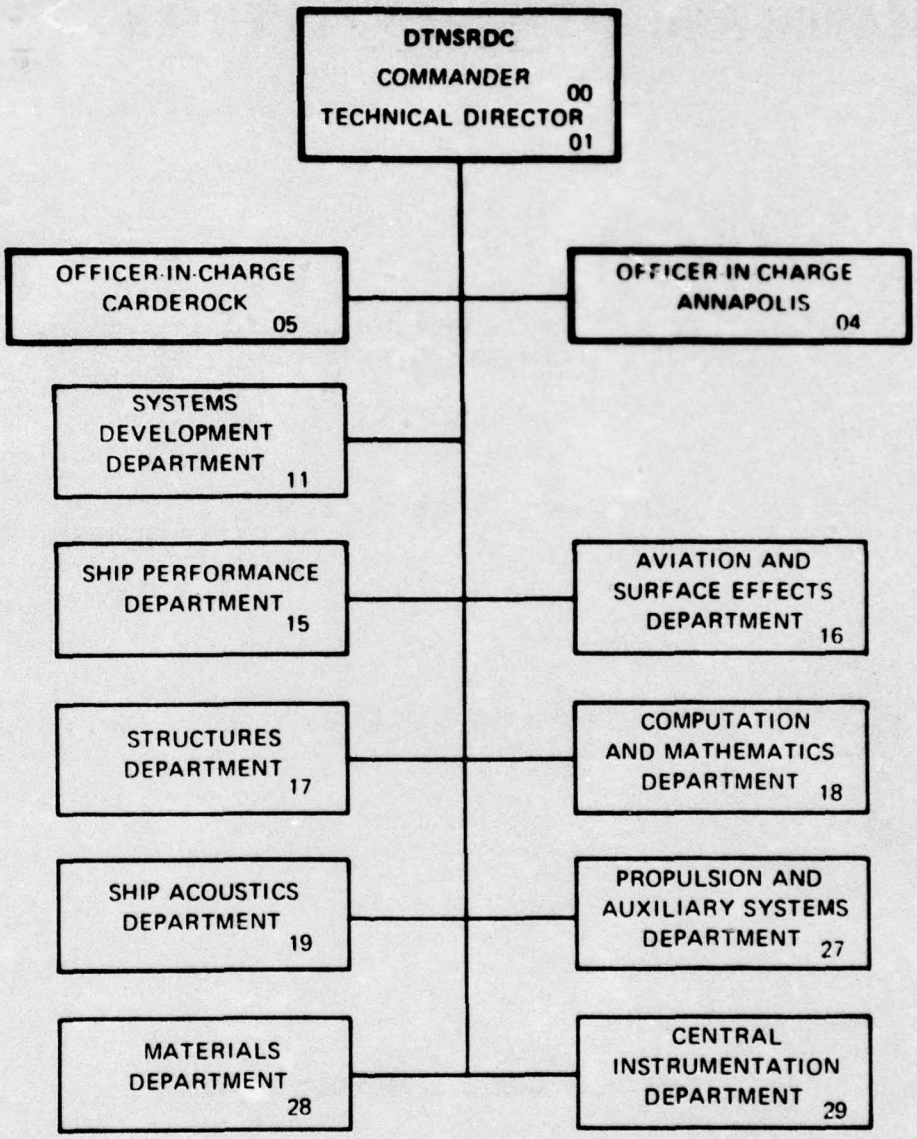

UNCLASSIFIED

SECURITY CLASSIFICATION OF THIS PAGE (When Data Entered)

REPORT DOCUMENTATION PAGE	READ INSTRUCTIONS BEFORE COMPLETING FORM
1. REPORT NUMBER (14) SPD-724-05 (6)	2. GOVT ACCESSION NO. / 3. RECIPIENT'S CATALOG NUMBER
4. TITLE (and Subtitle) ANALYSIS OF WAKE SURVEY DATA FOR A GUIDED MISSILE STRIKE CRUISER (CSGN) REPRESENTED BY MODEL 5352	5. TYPE OF REPORT & PERIOD COVERED (9) FINAL rept. / 6. PERFORMING ORG. REPORT NUMBER
7. AUTHOR(s) (10) ALAN C. M. LIN [redacted] RAE B. HURWITZ	8. CONTRACT OR GRANT NUMBER(s)
9. PERFORMING ORGANIZATION NAME AND ADDRESS DAVID W. TAYLOR NAVAL SHIP R&D CENTER BETHESDA, MD. 20084	10. PROGRAM ELEMENT, PROJECT, TASK AREA & WORK UNIT NUMBERS (12) 49p.
11. CONTROLLING OFFICE NAME AND ADDRESS NAVAL SHIP ENGINEERING CENTER WASHINGTON, D. C. 20362	12. REPORT DATE (11) DEC [redacted] 76 / 13. NUMBER OF PAGES 48
14. MONITORING AGENCY NAME & ADDRESS(if different from Controlling Office)	15. SECURITY CLASS. (of this report) UNCLASSIFIED / 15a. DECLASSIFICATION/DOWNGRADING SCHEDULE

16. DISTRIBUTION STATEMENT (of this Report)

APPROVED FOR PUBLIC RELEASE: DISTRIBUTION UNLIMITED

17. DISTRIBUTION STATEMENT (of the abstract entered in Block 20, if different from Report)

18. SUPPLEMENTARY NOTES

19. KEY WORDS (Continue on reverse side if necessary and identify by block number)

(U) Propeller design

20. ABSTRACT (Continue on reverse side if necessary and identify by block number)

The Naval Ship Engineering Center (NAVSEC) initiated a model experimental program at the David W. Taylor Naval Ship R&D Center (DTNSRDC) to aid in the evaluation of a proposed design of the Nuclear Guided Missile Strike Cruiser (CSGN). This report presents the results of the wake survey experiment performed in the plane of the propeller disk. The harmonic analyses of the circumferential distribution of the longitudinal and tangential velocities are also presented.

DD FORM 1 JAN 73 1473 EDITION OF 1 NOV 65 IS OBSOLETE S/N 0102-014-6601

389 694 UNCLASSIFIED

SECURITY CLASSIFICATION OF THIS PAGE (When Data Entered)

LIST OF FIGURES

LIST OF FIGURES (continued)

LIST OF FIGURES (continued)

LIST OF TABLES

NOTATION

CONVENTIONAL SYMBOL	SYMBOL APPEARING ON PLOTS	DEFINITION
A_N	COS COEF	The cosine coefficient of the N^{th} harmonic*
B_N	SIN COEF	The sine coefficient of the N^{th} harmonic*
D	----	Propeller diameter
J_a	----	Apparent advance coefficient $J_a = \frac{V}{nD}$ (dimensionless)
N	N	Harmonic number
n	----	Propeller revolutions
r/R or x	RADIUS or RAD.	Distance (r) from the propeller axis expressed as a ratio of the propeller radius (R)
V	V	Actual model or ship velocity
$V_b(x,\theta)$	----	Resultant inflow velocity to blade for a given point
$\overline{V}_b(x)$	----	Mean resultant inflow velocity to blade for a given radius
$V_r(x,\theta)$	VR	Radial component of the fluid velocity for a given point (positive toward the shaft centerline)
$\overline{V}_r(x)$	----	Mean radial velocity component for a given radius
$V_r(x,\theta)/V$	VR/V	Radial velocity component ratio for a given point
$\overline{V}_r(x)/V$	VRBAR	Mean radial velocity component ratio for a given radius
$V_t(x,\theta)$	VT	Tangential component of the fluid velocity for a given point (positive in a counterclockwise direction looking forward)

*See footnote on the following page

NOTATION (Continued)

$\overline{V}_t(x)$	----	Mean tangential velocity component for a given radius
$V_t(x,\theta)/V$	VT/V	Tangential velocity component ratio for a given point
$\overline{V}_t(x)/V$	VTBAR	Mean tangential velocity component ratio for a given radius
$(\widetilde{V}_t(x)/V)_N$	AMPLITUDE	Amplitude (B_N for single screw symmetric; C_N otherwise) of Nth harmonic of the tangential velocity component ratio for a given radius*
$V_x(x,\theta)$	VX	Longitudinal (normal to the plane of survey) component of the fluid velocity for a given point (positive in the astern direction)
$\overline{V}_x(x)$	----	Mean longitudinal velocity component for a given radius
$V_x(x,\theta)/V$	VX/V	Longitudinal velocity component ratio for a given point
$\overline{V}_x(x)/V$	VXBAR	Mean longitudinal velocity component ratio for a given radius
$(\widetilde{V}_x(x)/V)_N$	AMPLITUDE	Amplitude (A_N for single screw symmetric; C_N otherwise) of Nth harmonic of the longitudinal velocity component ratio for a given radius*
ϕ_N	PHASE ANGLE	Phase Angle of Nth harmonic*

*The harmonic amplitudes of any circumferential velocity distribution $f(\theta)$ are the coefficients of the Fourier Series:

$$f(\theta) = A_o + \sum_{N=1}^{NH} A_N \cos(N\theta) + \sum_{N=1}^{NH} B_N \sin(N\theta)$$

$$= A_o + \sum_{N=1}^{NH} C_N \sin(N\theta + \phi_N)$$

1-w(x)	1 - WX	Volumetric mean velocity ratio from the hub to a given radius

$$1\text{-}w(r/R) = \left[\frac{2 \cdot \int_{r_{hub}/R}^{r/R} (V_{x_c}(x)/V) \cdot x \cdot dx}{(r/R)^2 - (r_{hub}/R)^2} \right]$$

where $$V_{x_c}(x)/V = \int_0^{2\pi} \left[\frac{V_{x_c}(x,\theta)}{2\pi V} \right] d\theta$$

and $$(V_{x_c}(x,\theta)/V) = (V_x(x,\theta)/V) - (V_t(x,\theta)/V) \tan(\beta(x,\theta))$$

1-w(x)	1-WVX	Volumetric mean velocity ratio from the hub to a given radius (without the tangential velocity correction)

$$1\text{-}w(r/R) = \left[\frac{2 \cdot \int_{r_{hub}/R}^{r/R} (\bar{V}_x(x)/V) \cdot x \cdot dx}{(r/R)^2 - (r_{hub}/R)^2} \right]$$

$\beta(x,\theta)$	----	Advance angle in degrees for a given point
$\bar{\beta}(x)$	BBAR	Mean advance angle in degrees for a given radius

NOTATION (Continued)

$+\Delta\beta$	BPOS	Variation of the maximum advance angle from the mean for a given radius
$-\Delta\beta$	BNEC	Variation of the minimum advance angle from the mean for a given radius
θ	ANGLE IN DEGREES	Position angle (angular coordinate) in degrees

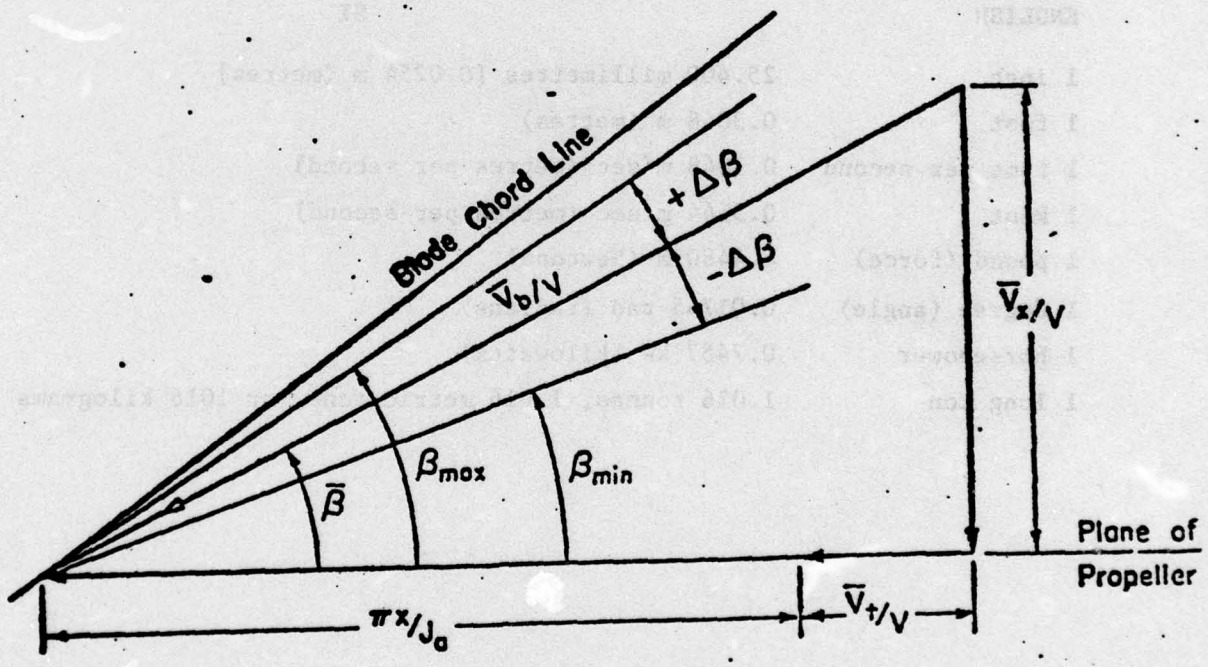

ENGLISH/SI EQUIVALENTS

ENGLISH	SI
1 inch	25.400 millimetres [0.0254 m (metres]
1 foot	0.3048 m (metres)
1 foot per second	0.3048 m/sec (metres per second)
1 knot	0.5144 m/sec (metres per second)
1 pound (force)	4.4480 N (Newtons)
1 degree (angle)	0.01745 rad (radians)
1 horsepower	0.7457 kW (kilowatts)
1 long ton	1.016 tonnes, 1.016 metric tons, or 1016 kilograms

INTRODUCTION

The Naval Ship Engineering Center (NAVSEC) initiated a model experimental program at the David W. Taylor Naval Ship Research and Development Center (DTNSRDC) to aid in the evaluation of a proposed design of the Nuclear Guided Missile Strike Cruiser (CSGN). This report presents the results of the wake survey experiment performed in the plane of the propeller disk. The harmonic analyses of the circumferential distribution of the longitudinal and tangential velocities are also presented. Separate reports associated with this experimental program have been issued.

EXPERIMENTAL PROCEDURE AND PRESENTATION OF DATA

DTNSRDC Model 5352, representing a conventional hull form of CSGN design, was constructed to a linear ratio of 24 in accordance with NAVSEC's model plans.[1,2] The model was fitted with appendages except for the rudders. The velocity survey was conducted at the design draft of 22.15 feet (6.751 m), even keel in the static condition, at a displacement of 17,050 tons (17320 tonne) full scale, and at a velocity representing a ship speed of 30 knots (15.432 m/s).

A pitot tube rake, DTNSRDC No. 7, and four differential pressure gages were used to measure the velocities in the plane of the propeller disk at five radial locations. The pitot tube rake consisted of five 5-hole

spherical pitot tubes mounted in a housing. Figure 1 shows this arrangement and Figure 2 shows the pitot tube rake, mounted in the port shaft of the model.

The full scale propeller disk was 18 feet (5.488 m) in diameter. The radii at which the measurements were made were expressed as ratios of the propeller radius (r/R), and were 0.338, 0.524, 0.729, 0.933 and 1.109 as shown in Figure 3. The propeller plane in which the velocity measurements were taken was 2 feet (0.61 m) forward of station 19. To ensure the proper trim throughout the experiments, the model was towed at the corresponding design displacement of 17,050 tons (17320 tonne) and a ship speed of 30 knots (15.432 m/s) with the rake in the zero-degree position. The model was then locked and tested at this trimmed condition throughout the experiment.

Circumferential distribution of the longitudinal, tangential, and radial velocity component ratios are shown in graphical form for each tube radius in Figures 4 through 8. The mean longitudinal (VXBAR), tangential (VTBAR), and radial (VRBAR) component ratios of the velocity-vectors and volumetric mean wake velocity ratio ($1-w_X$) are presented in Table 1. These quantities, except the radial component (VRBAR) are shown graphically in Figure 9.

The calculated mean values of the advance angle (BBAR), and the maximum variations thereof, (BPOS) and (BNEG), are given in Figure 10 and Table 1. The advance angles were calculated using an advance coefficient, J_a, of 1.051. A diagram showing the relationship between the longitudinal and tangential velocity vectors, the advance coefficients and the advance angles is described on page ix .

Tables 2 through 5 present the harmonic analyses of the circumferential distributions of the longitudinal and tangential velocity component ratios at the experimental and interpolated radii. The amplitudes and phase angles of the ten harmonics of the longitudinal and tangential velocities are plotted graphically in Figures 11 through 30.

DISCUSSION

Data from this experiment has been compared with data from a typical twin-screw destroyer. The comparison showed that the results reported herein for the CSGN are reasonable, and in addition that the average effective wake factor ($\frac{(1-w_T) + (1-w_Q)}{2} = 0.949$) from the propulsion experiment is consistent with the volumetric mean wake velocity ($1-w_X = 0.936$ at 1.0 propeller radius) from this wake experiment. Therefore, this experiment is considered valid.

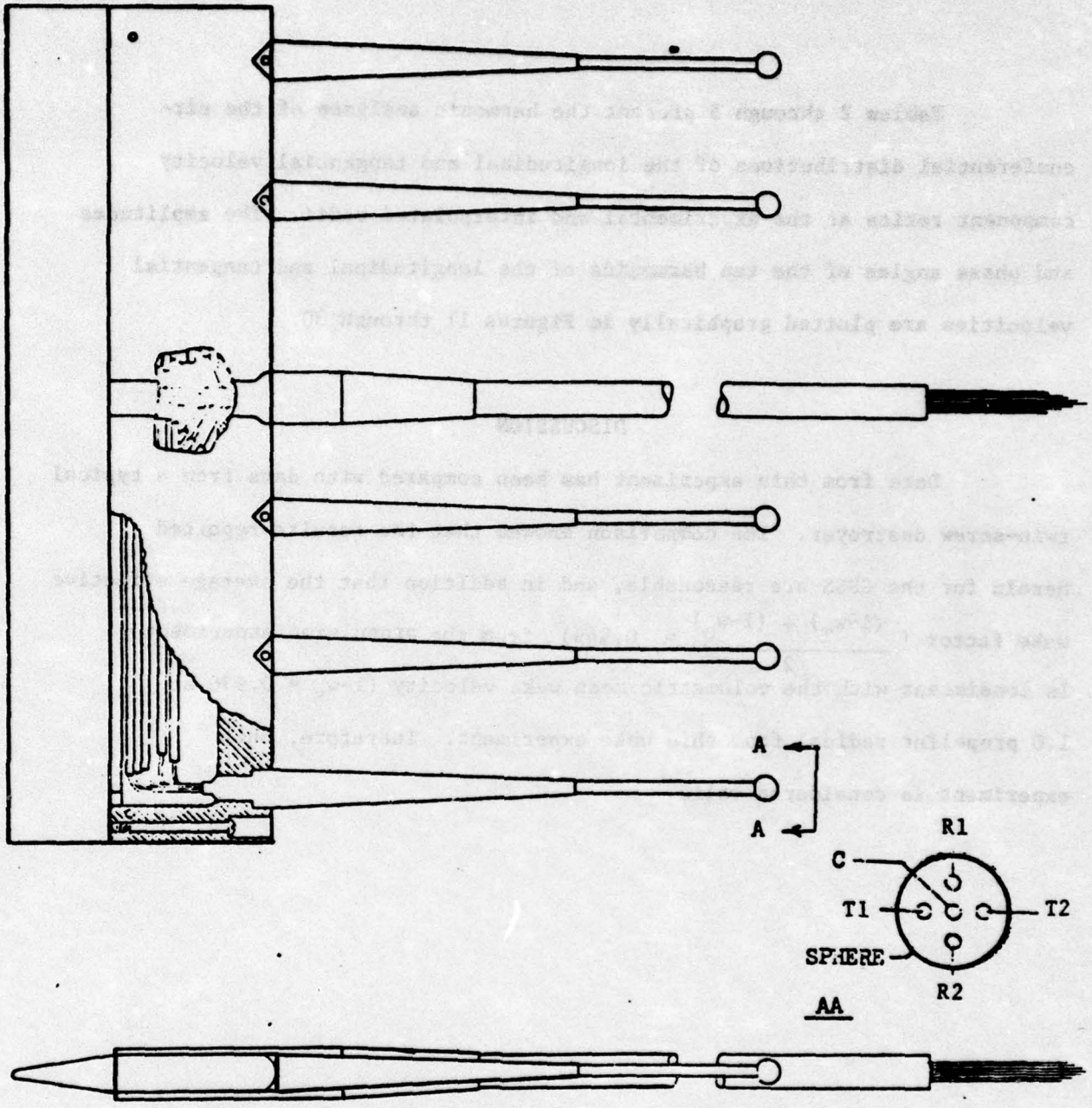

Figure 1 - Rake Arrangement Showing Spherical Head Pitot Tubes

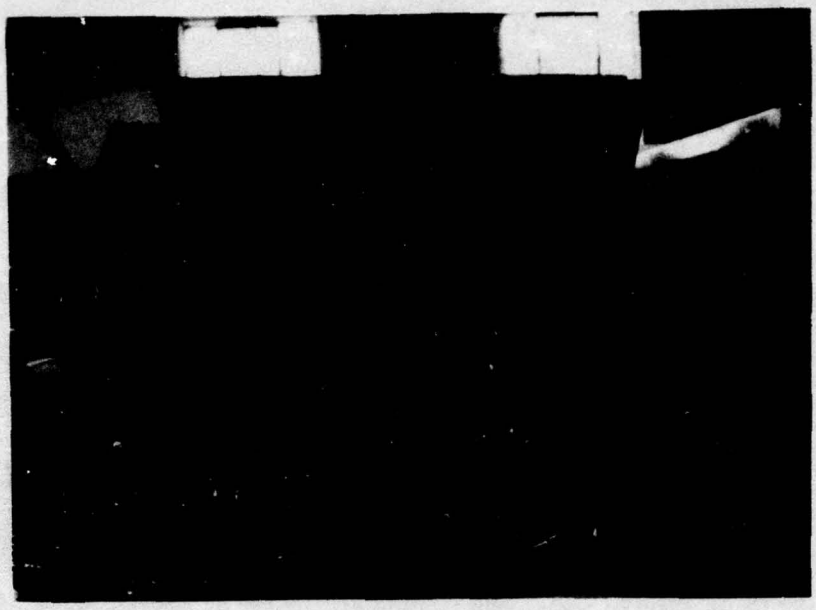

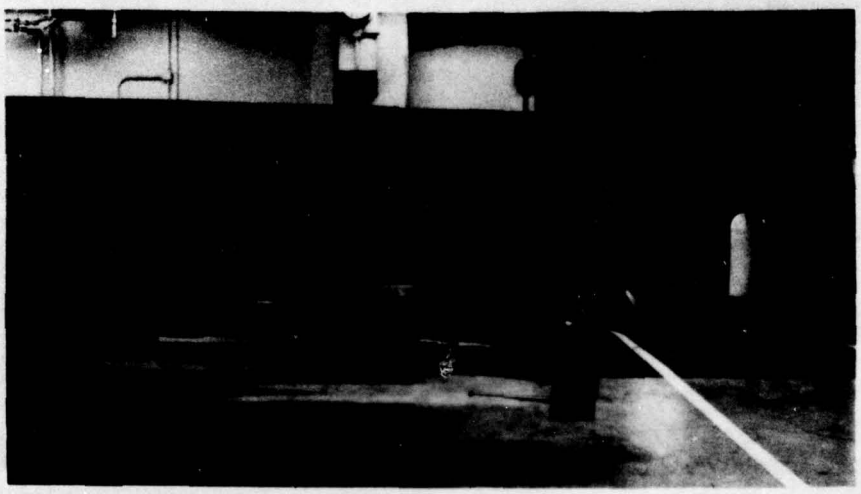

Figure 2 - Stern Views of the Pitot Tube Rake at the Propeller Disk Position on Model 5352 Representing the Conventional Hull Form CSGN

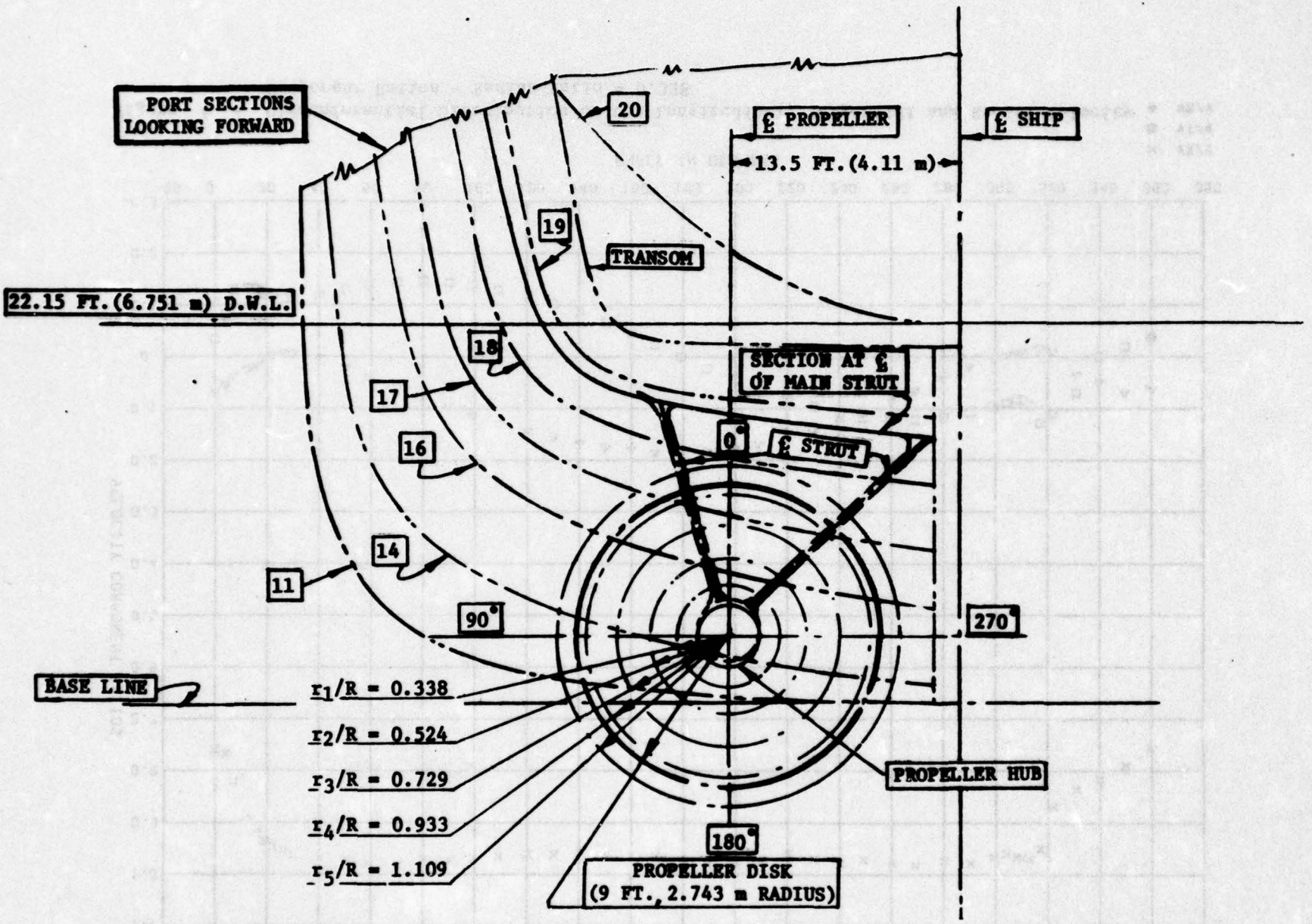

Figure 3 - Sectional View of the Experimental Radii in the Plane of Propeller Disk

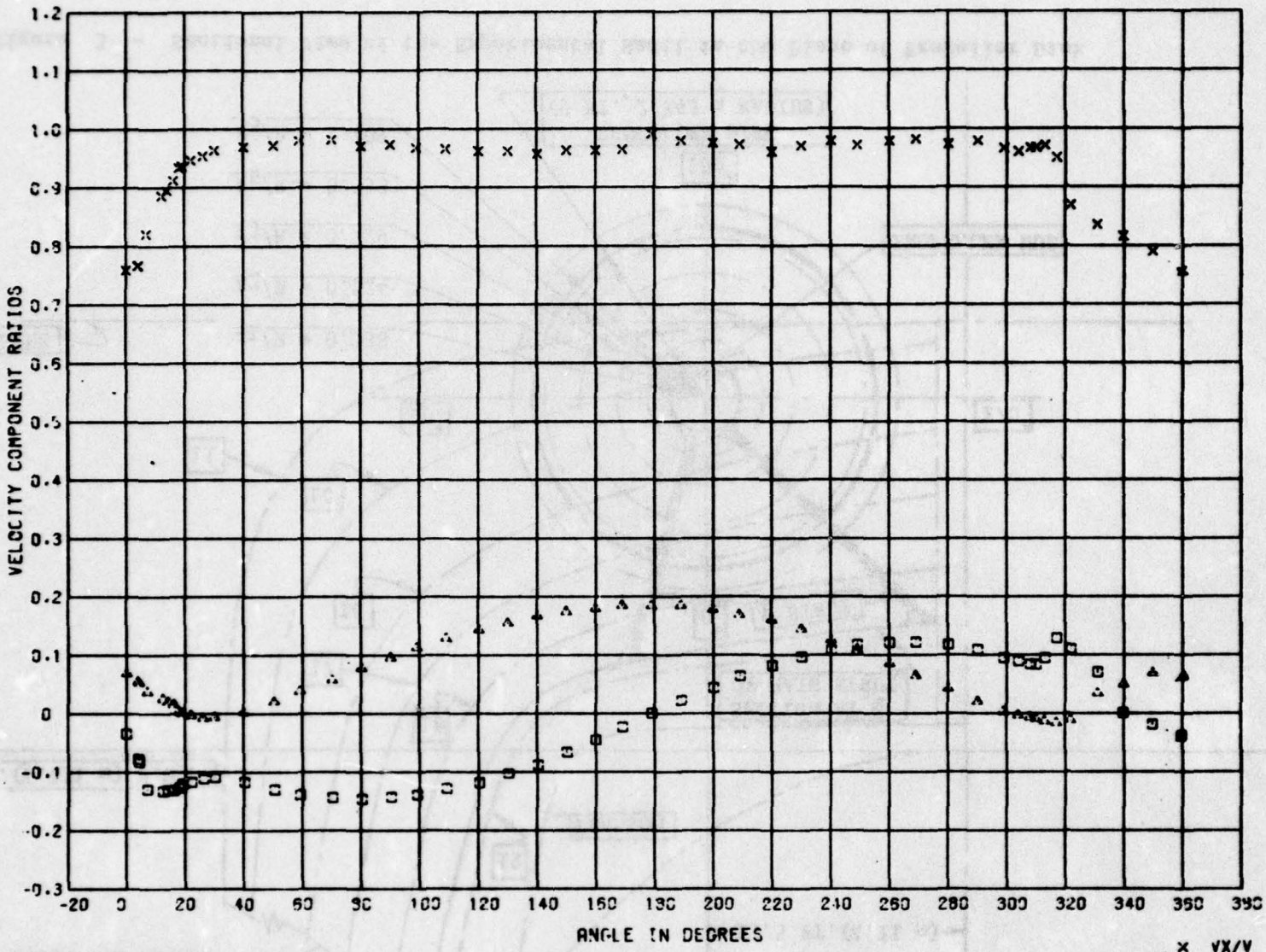

Figure 4 - Circumferential Distribution of the Longitudinal, Tangential and Radial Velocity Component Ratios - Radius Ratio = 0.338

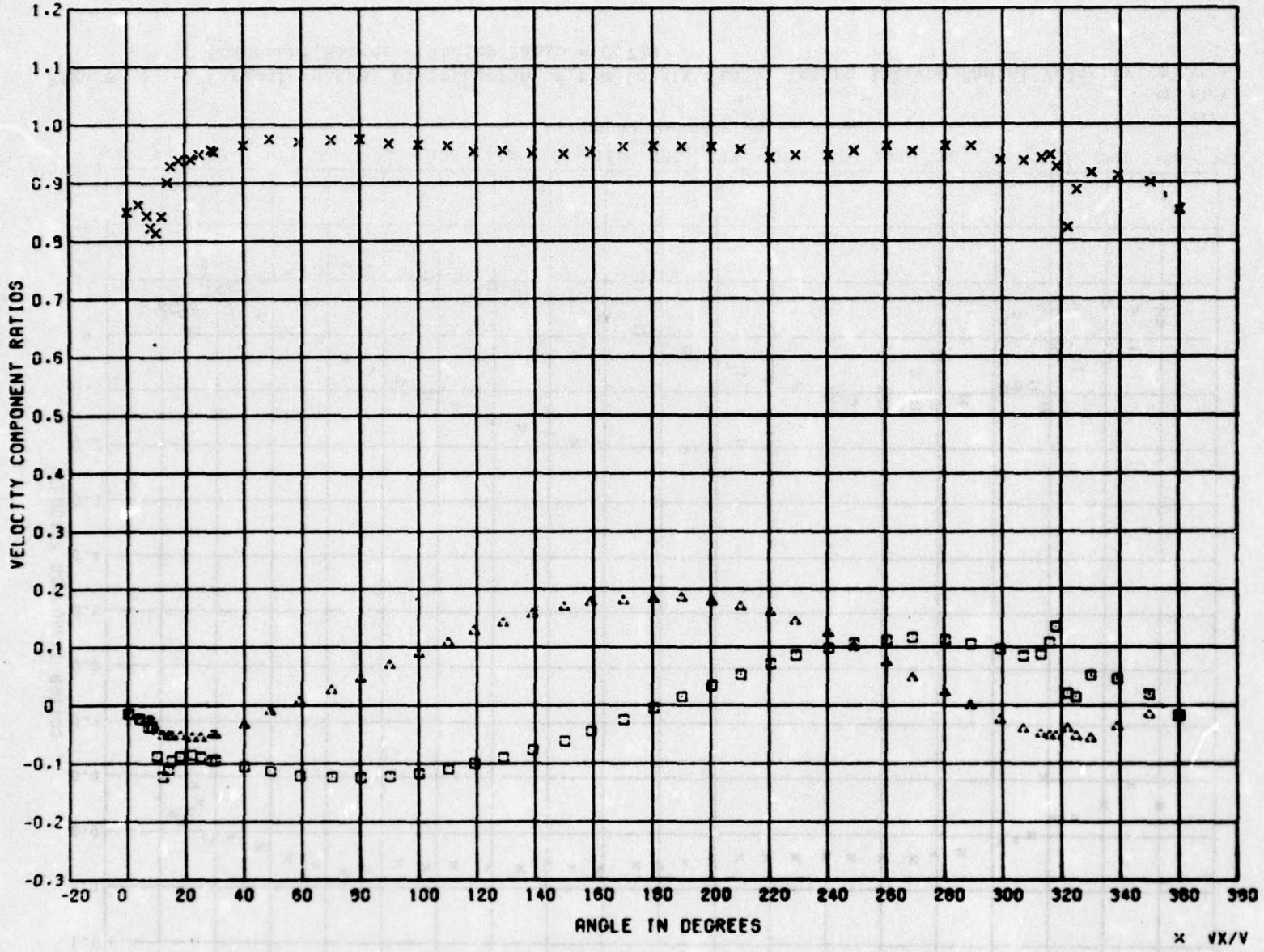

Figure 5 - Circumferential Distribution of the Longitudinal, Tangential and Radial Velocity Component Ratios - Radius Ratio = 0.524

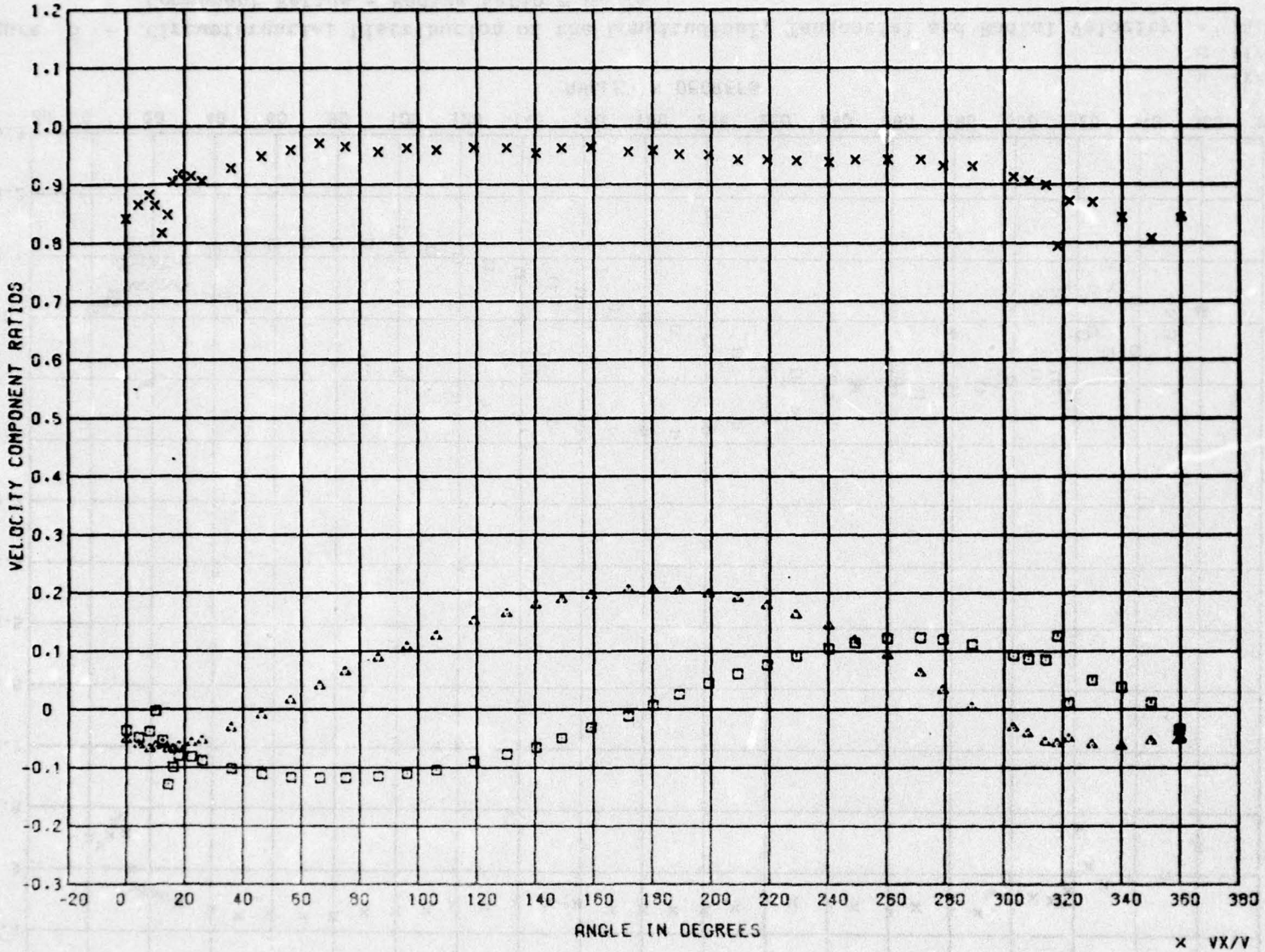

Figure 6 - Circumferential Distribution of the Longitudinal, Tangential and Radial Velocity Component Ratios - Radius Ratio = 0.729

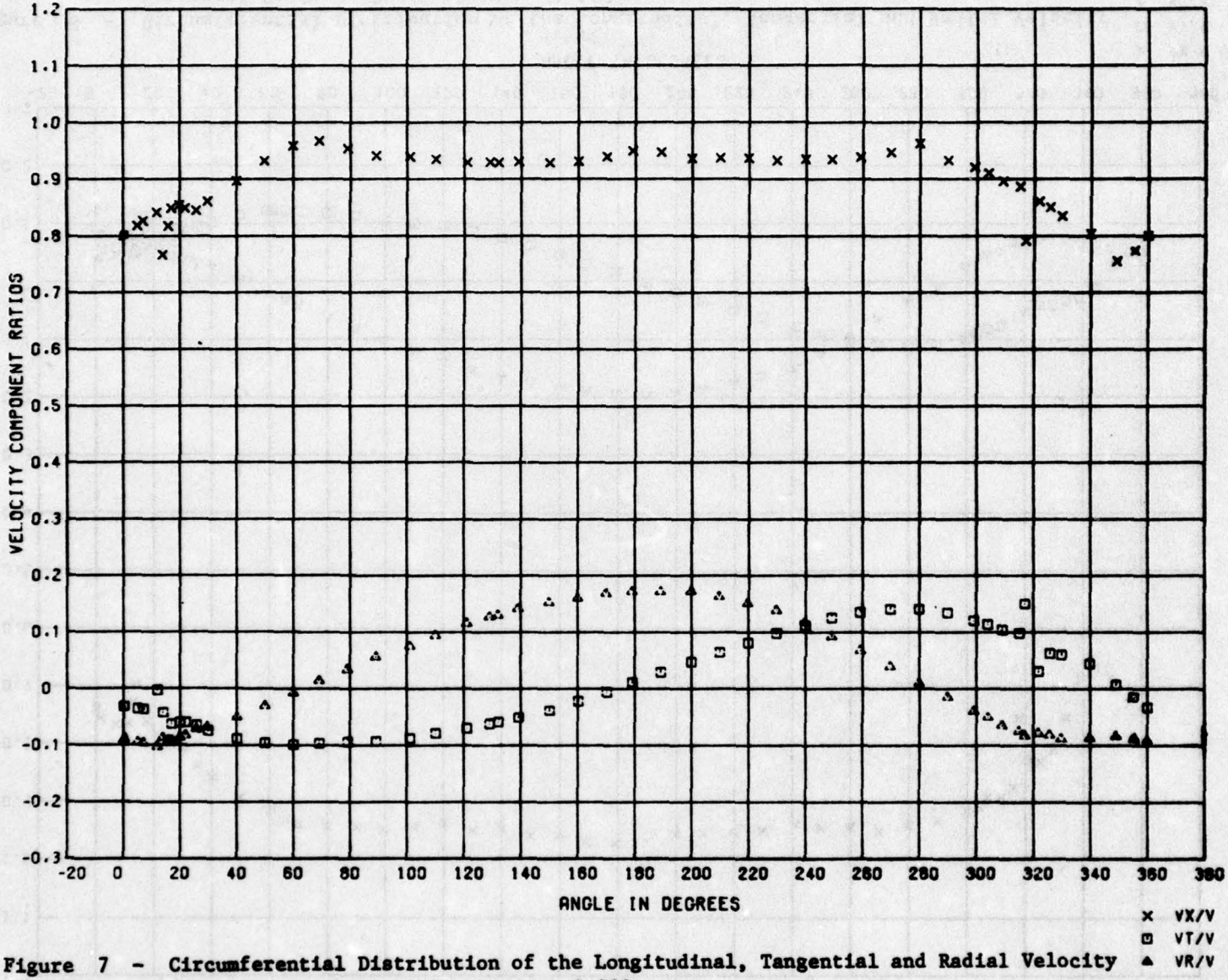

Figure 7 - Circumferential Distribution of the Longitudinal, Tangential and Radial Velocity Component Ratios - Radius Ratio = 0.933

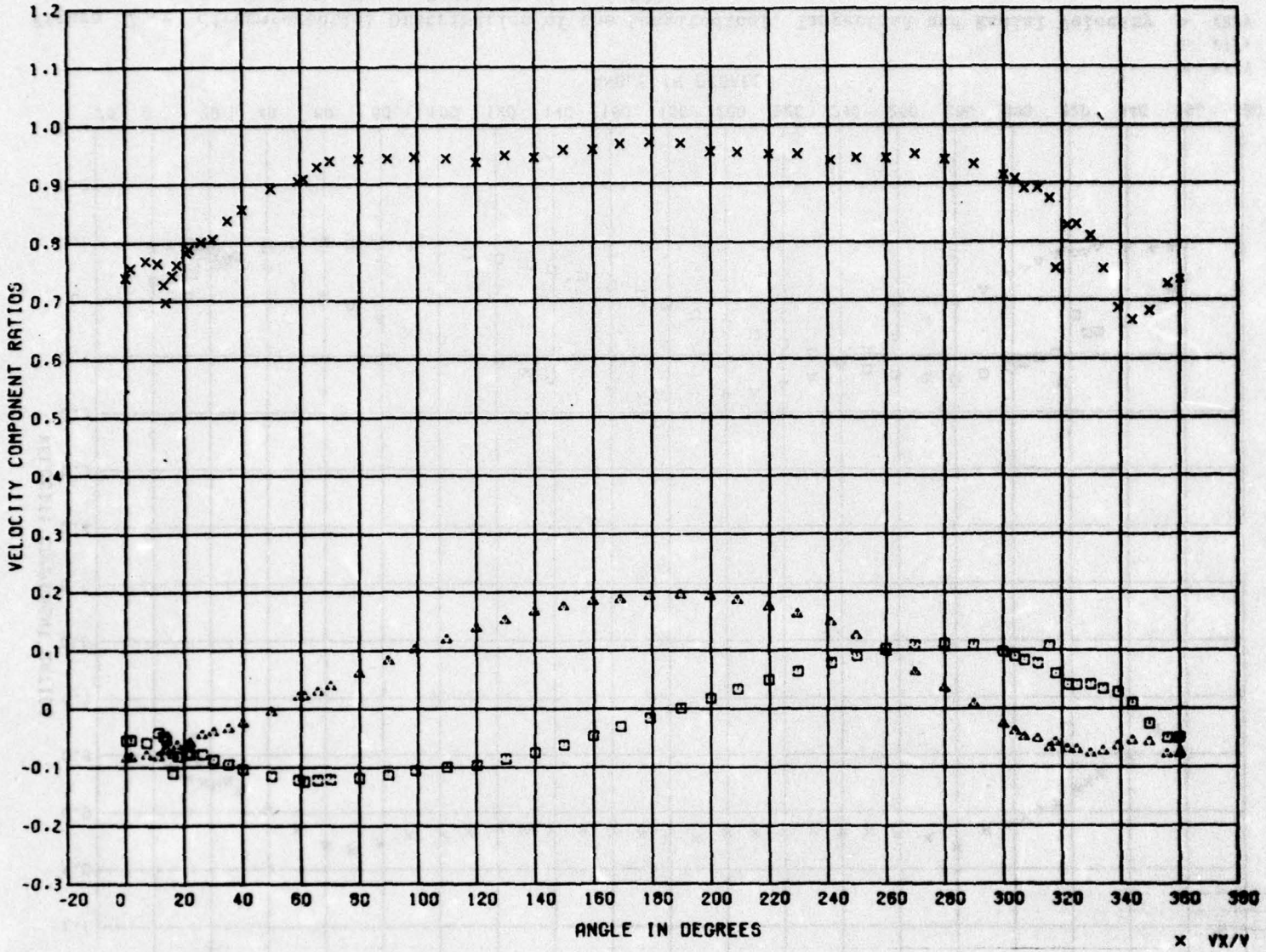

Figure 8 - Circumferential Distribution of the Longitudinal, Tangential and Radial Velocity Component Ratios - Radius Ratio = 1.109

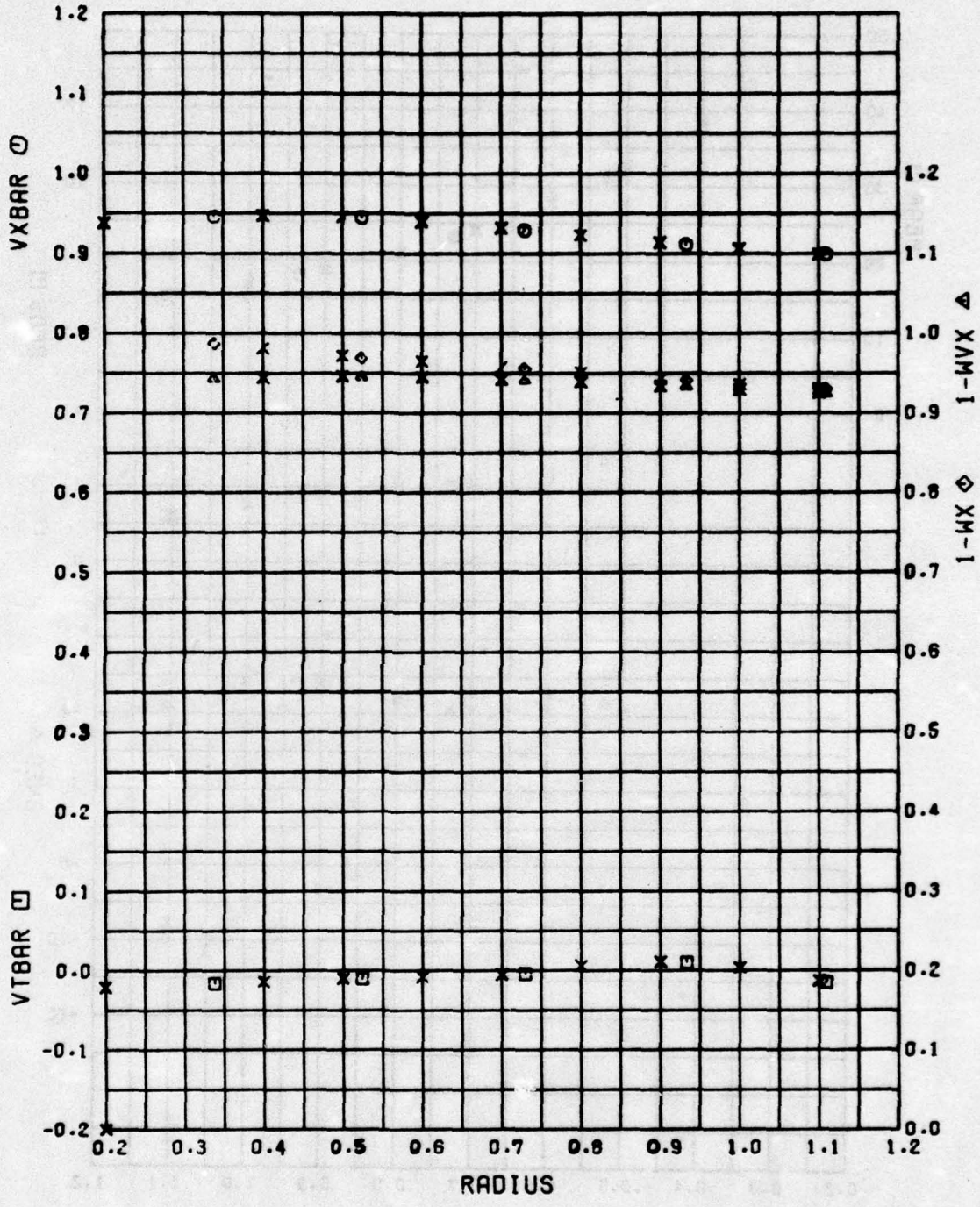

Figure 9 - Radial Distribution of the Mean Velocity Component Ratios

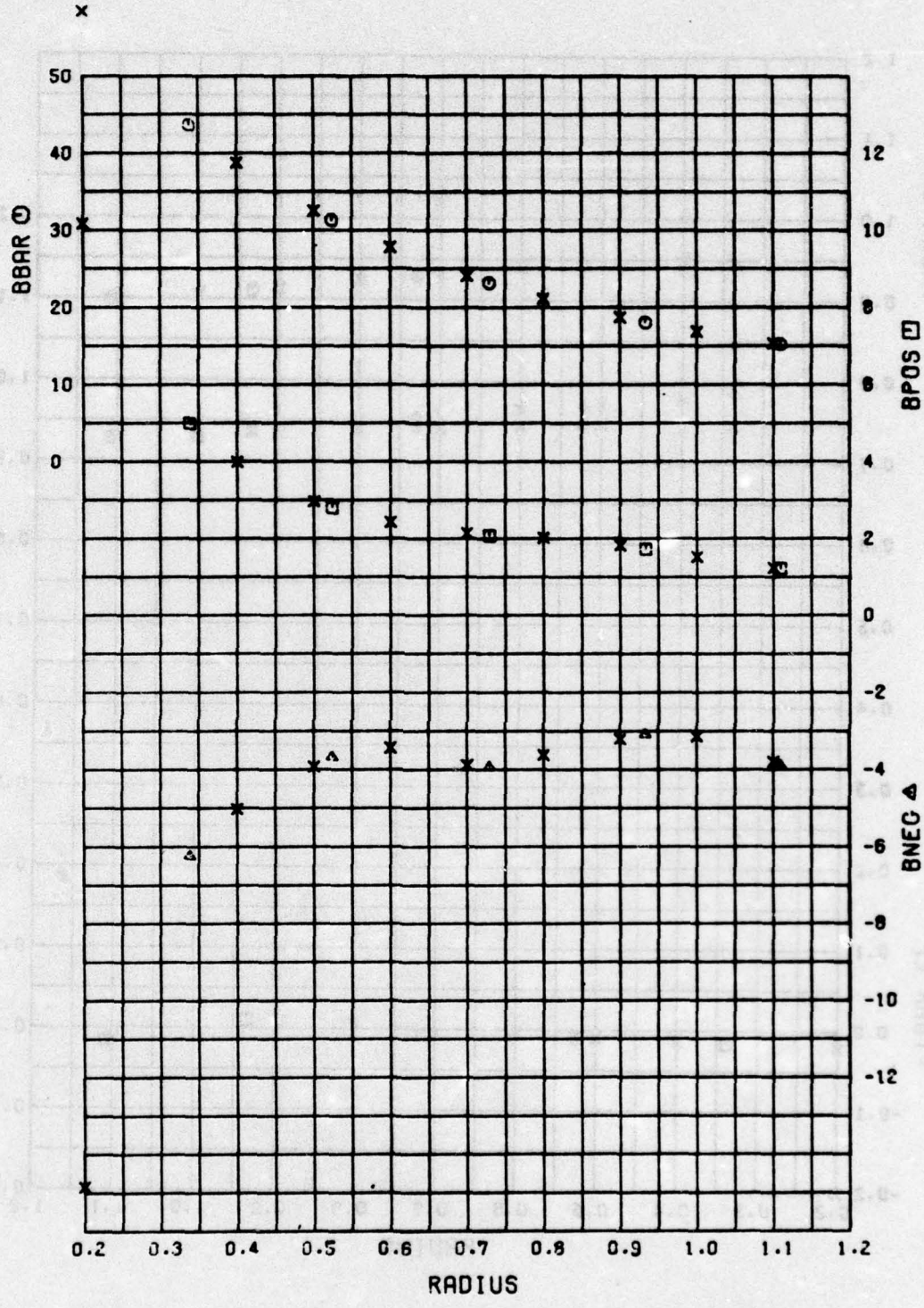

Figure 10 - Radial Distribution of the Mean Advance Angle and Other Derived Quantities

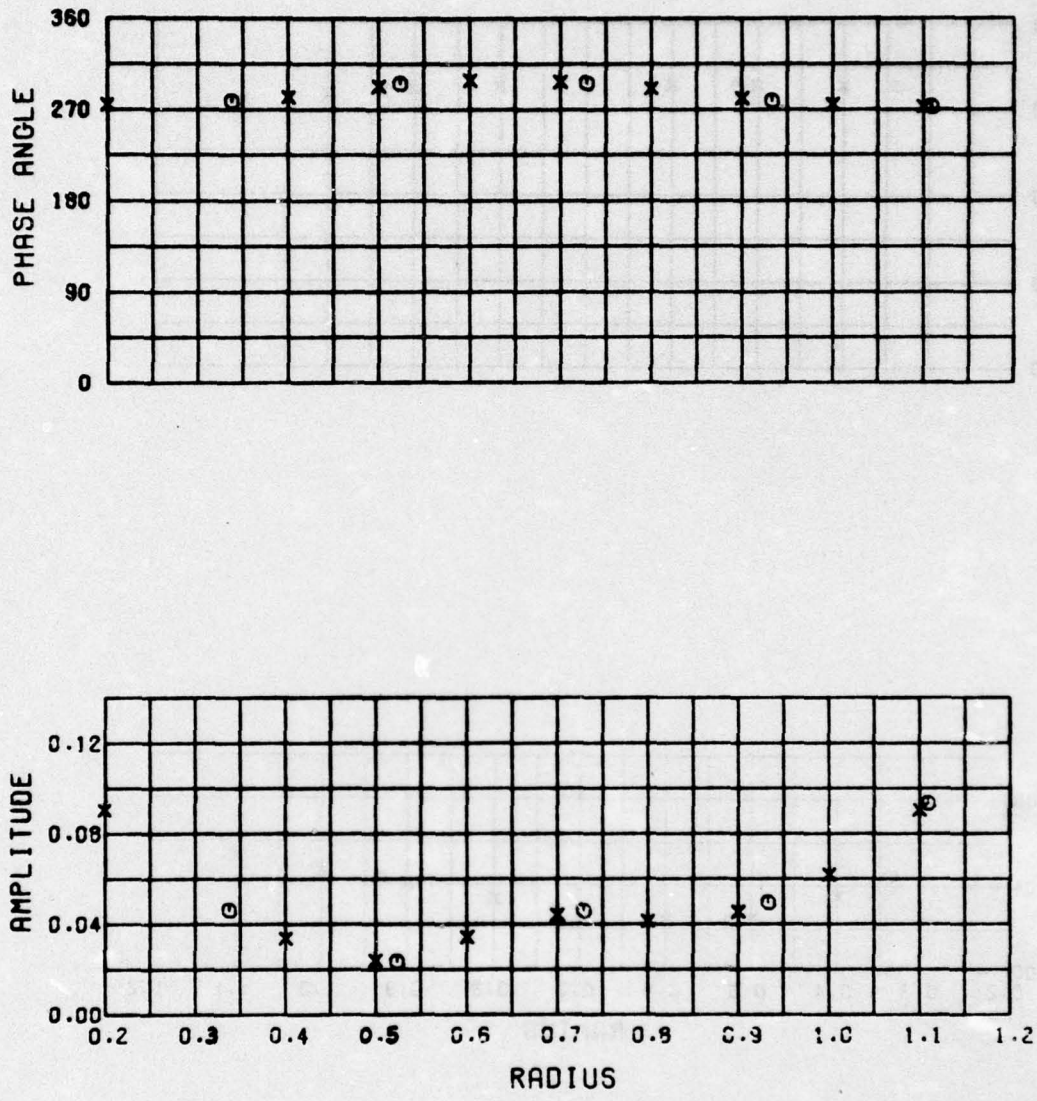

Figure 11 - Radial Distribution of the Amplitude and Phase Angle of the 1st Harmonic of the Circumferential Distribution of the Longitudinal Velocity Component Ratios

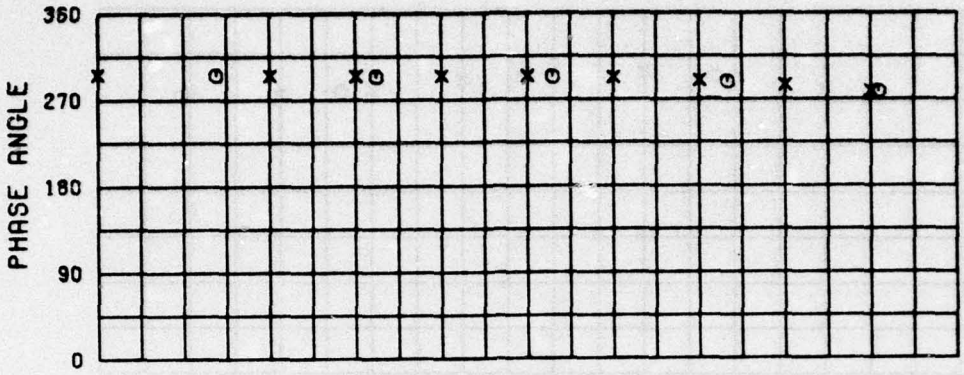

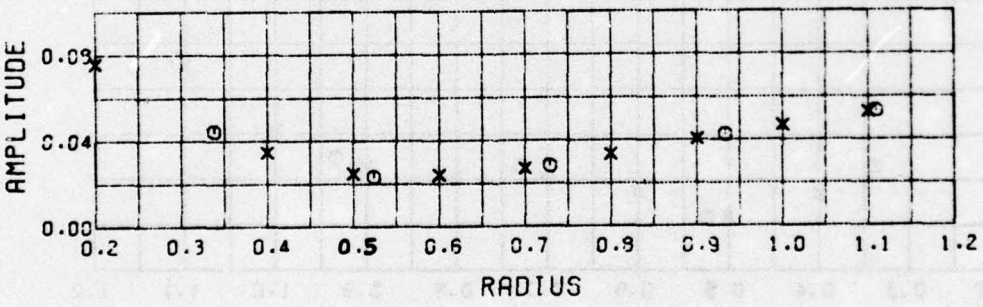

N = 2 VX/V

Figure 12 - Radial Distribution of the Amplitude and Phase Angle of the 2nd Harmonic of the Circumferential Distribution of the Longitudinal Velocity Component Ratios

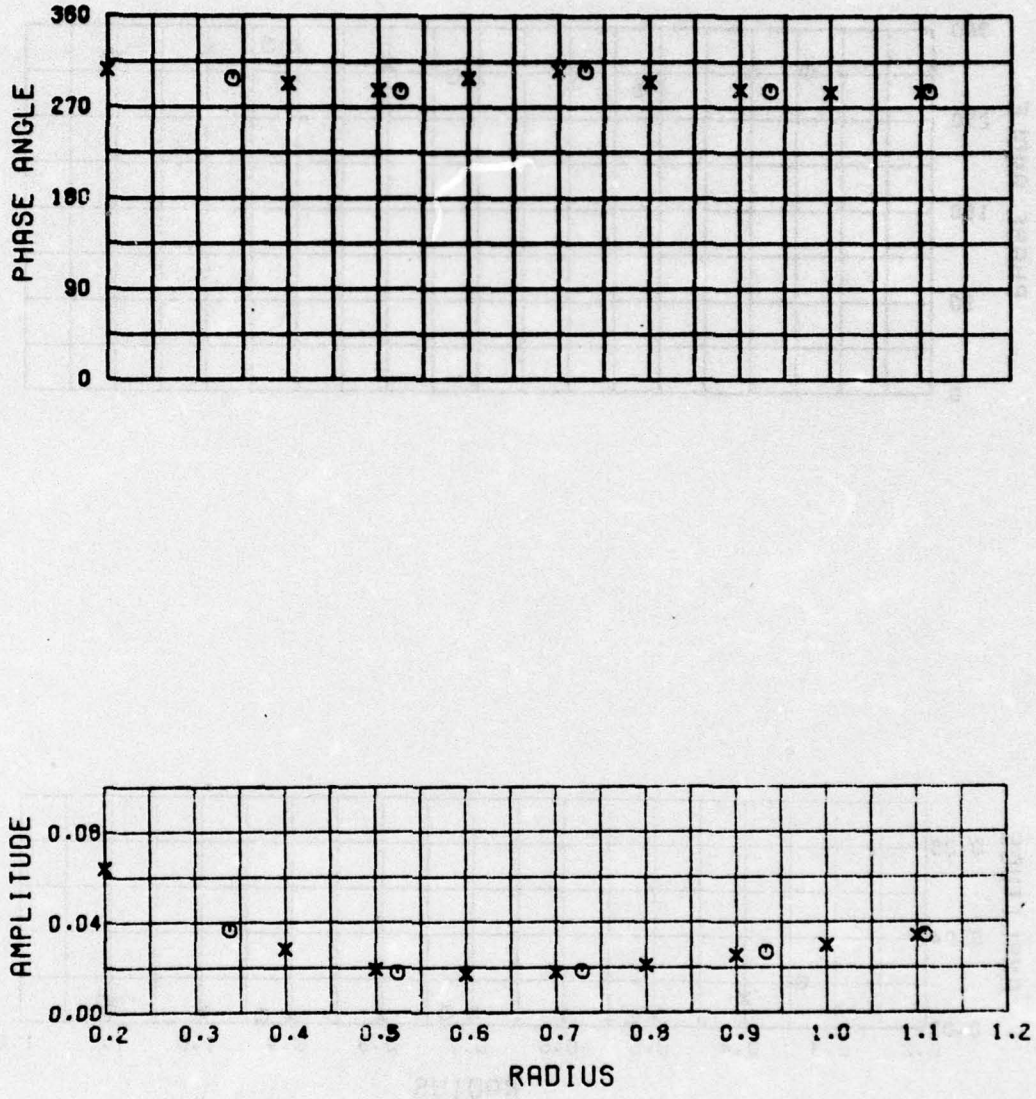

Figure 13 - Radial Distribution of the Amplitude and Phase Angle of the 3rd Harmonic of the Circumferential Distribution of the Longitudinal Velocity Component Ratios

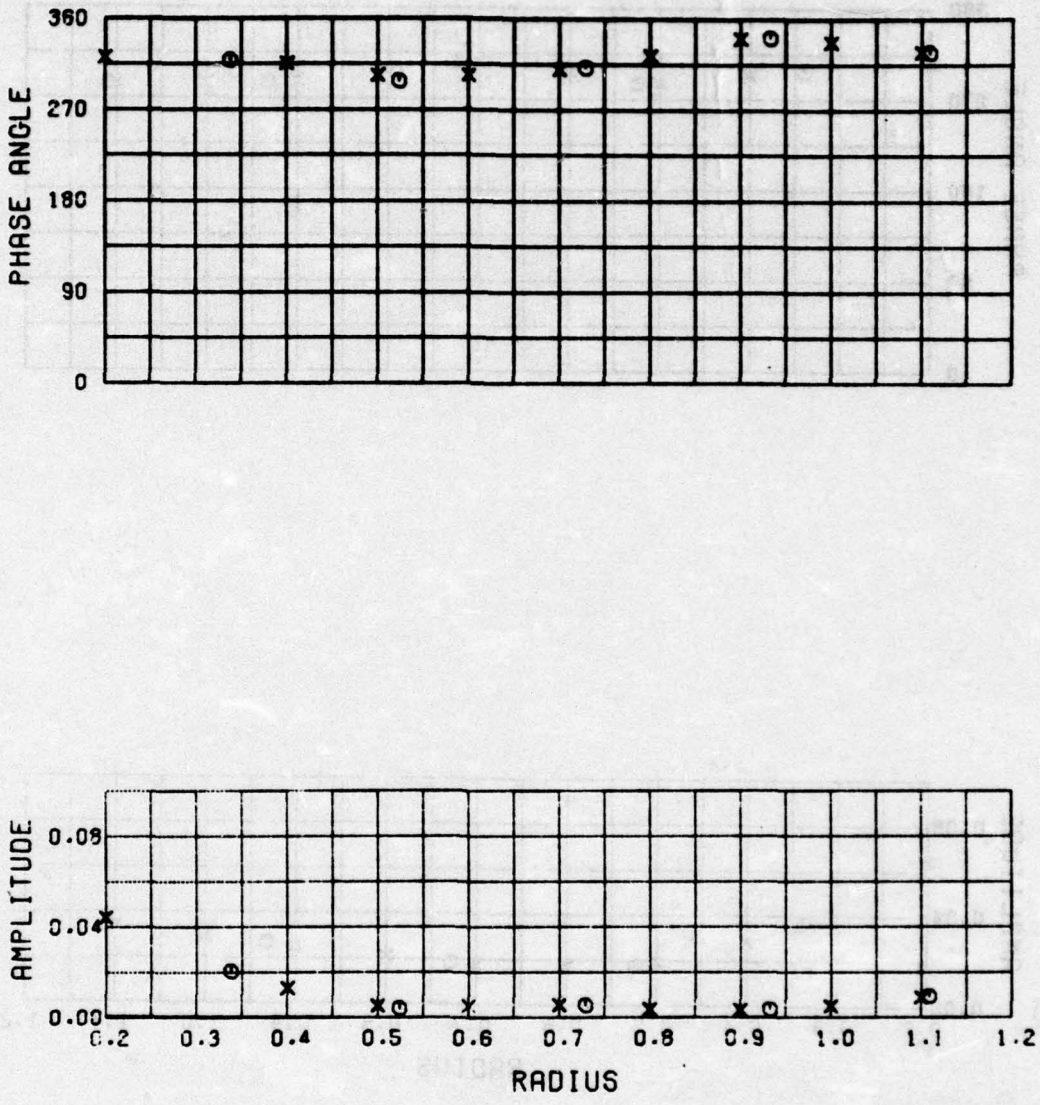

Figure 14 - Radial Distribution of the Amplitude and Phase Angle of the 4th Harmonic of the Circumferential Distribution of the Longitudinal Velocity Component Ratios

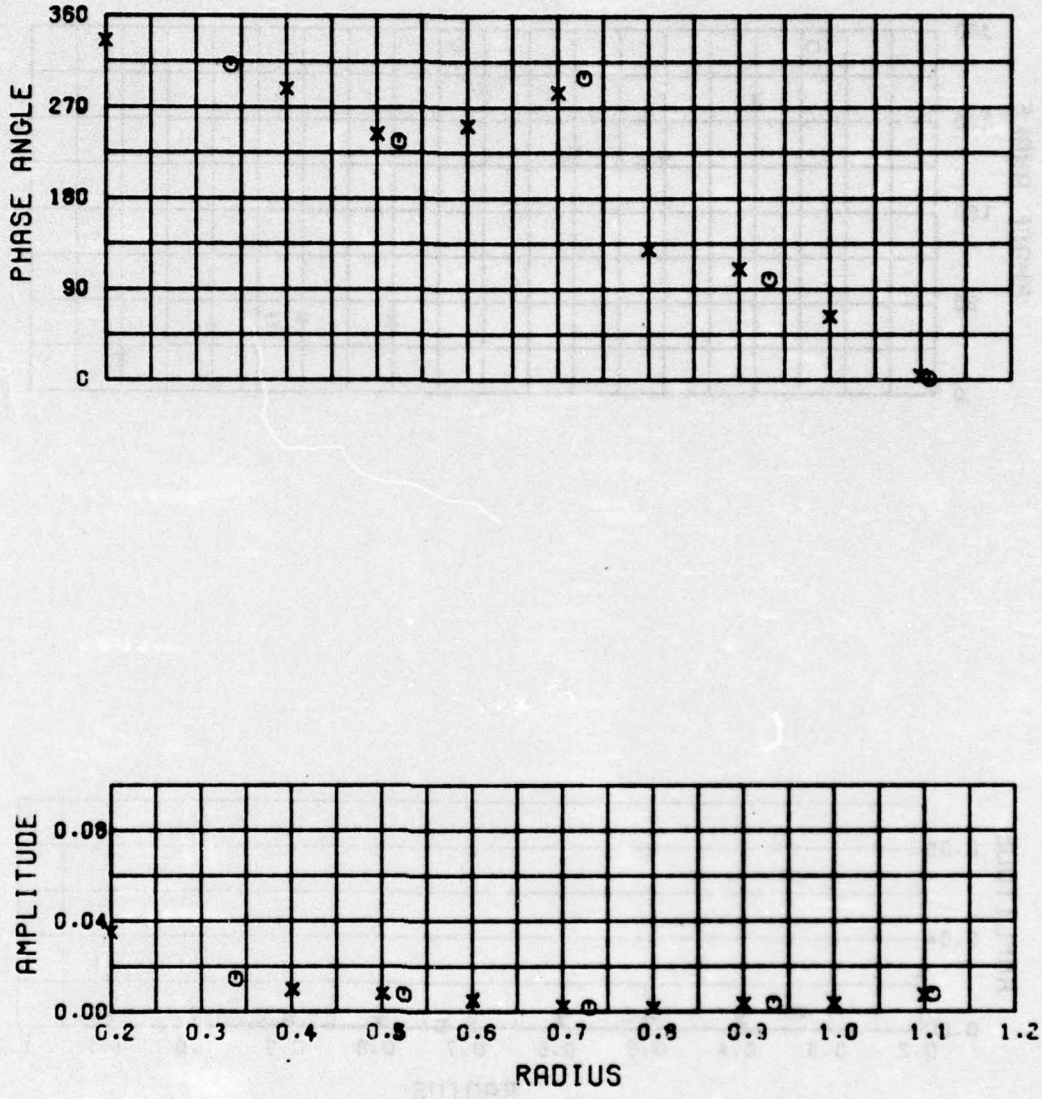

Figure 15 - Radial Distribution of the Amplitude and Phase Angle of the 5th Harmonic of the Circumferential Distribution of the Longitudinal Velocity Component Ratios

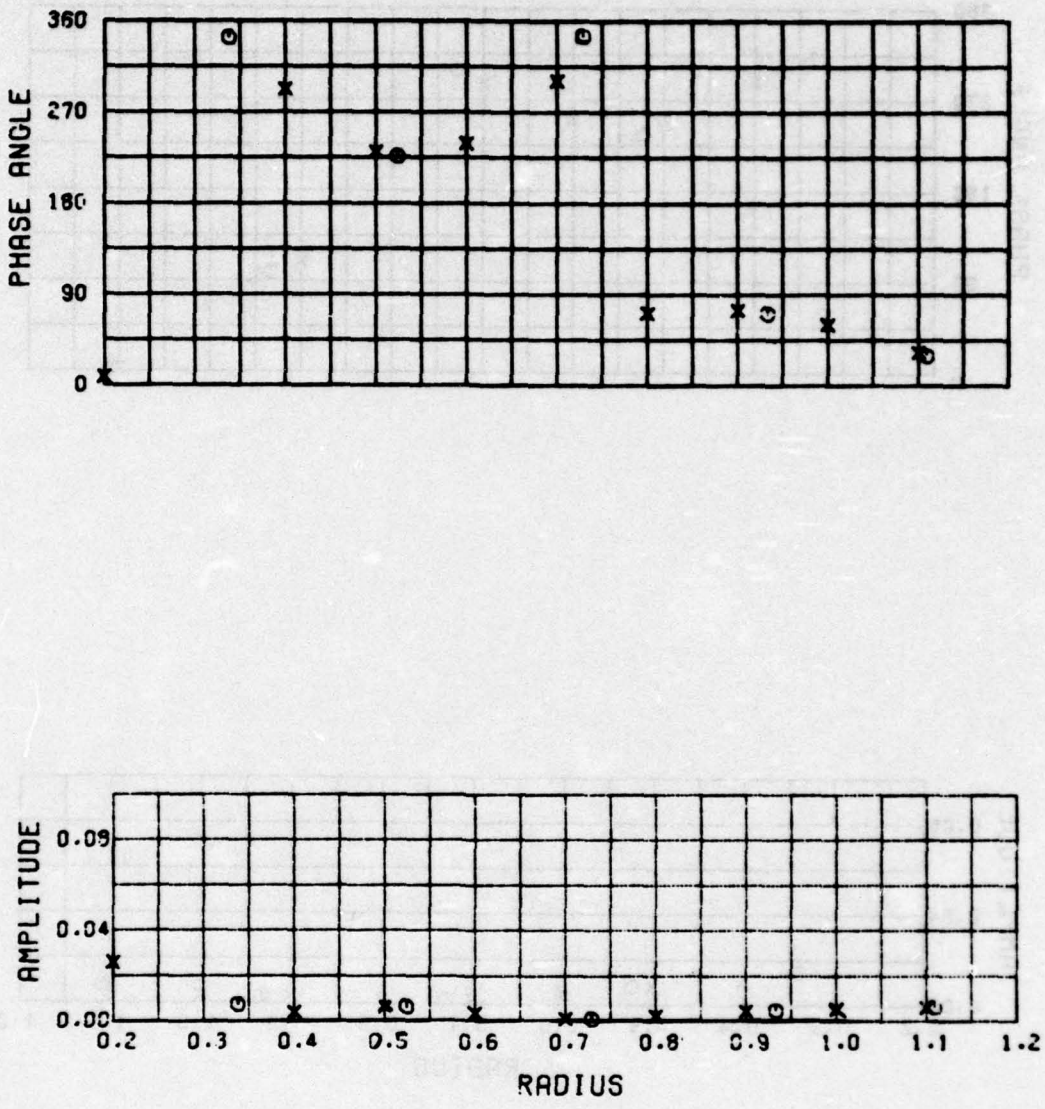

Figure 16 - Radial Distribution of the Amplitude and Phase Angle of the 6th Harmonic of the Circumferential Distribution of the Longitudinal Velocity Component Ratios.

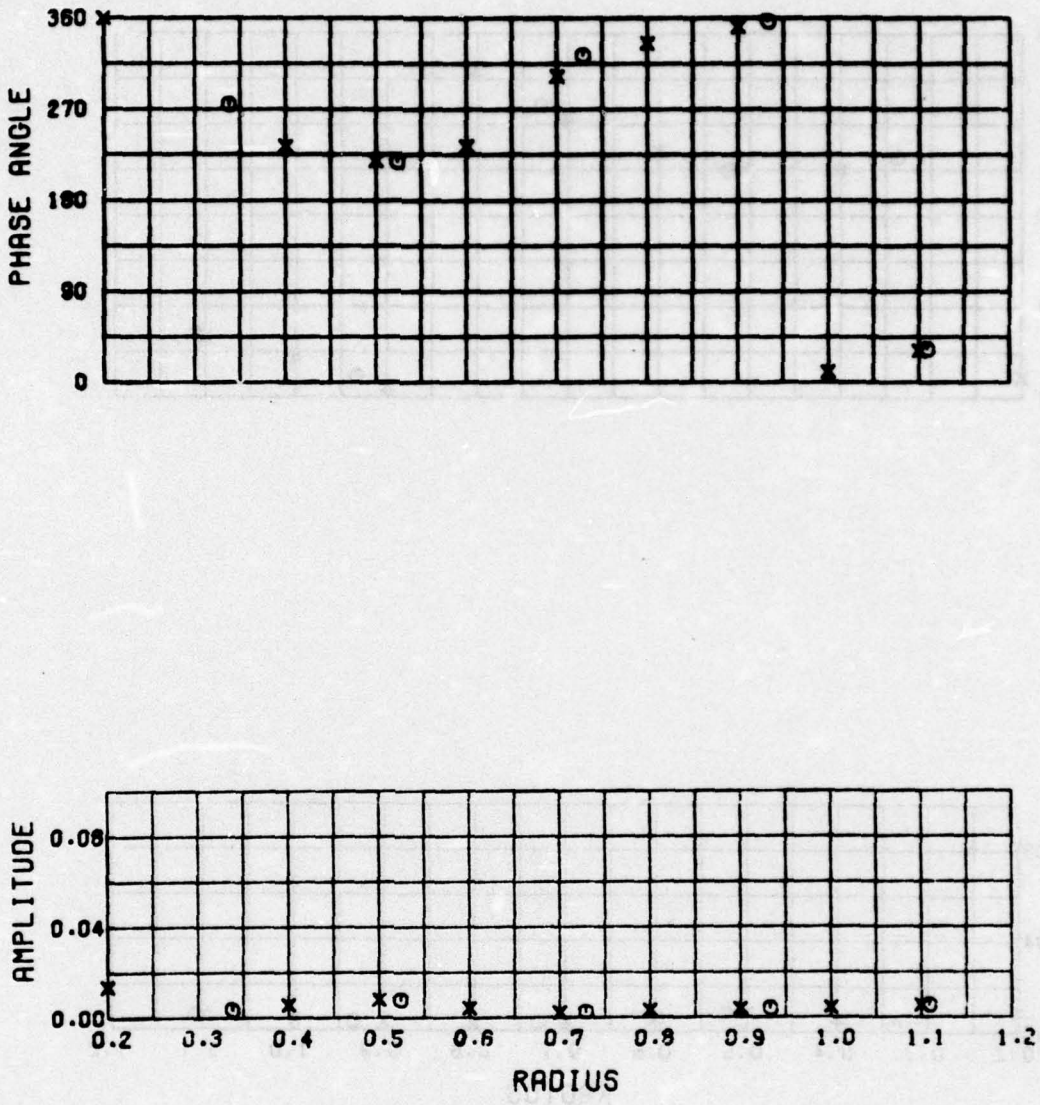

Figure 17 - Radial Distribution of the Amplitude and Phase Angle of the 7th Harmonic of the Circumferential Distribution of the Longitudinal Velocity Component Ratios

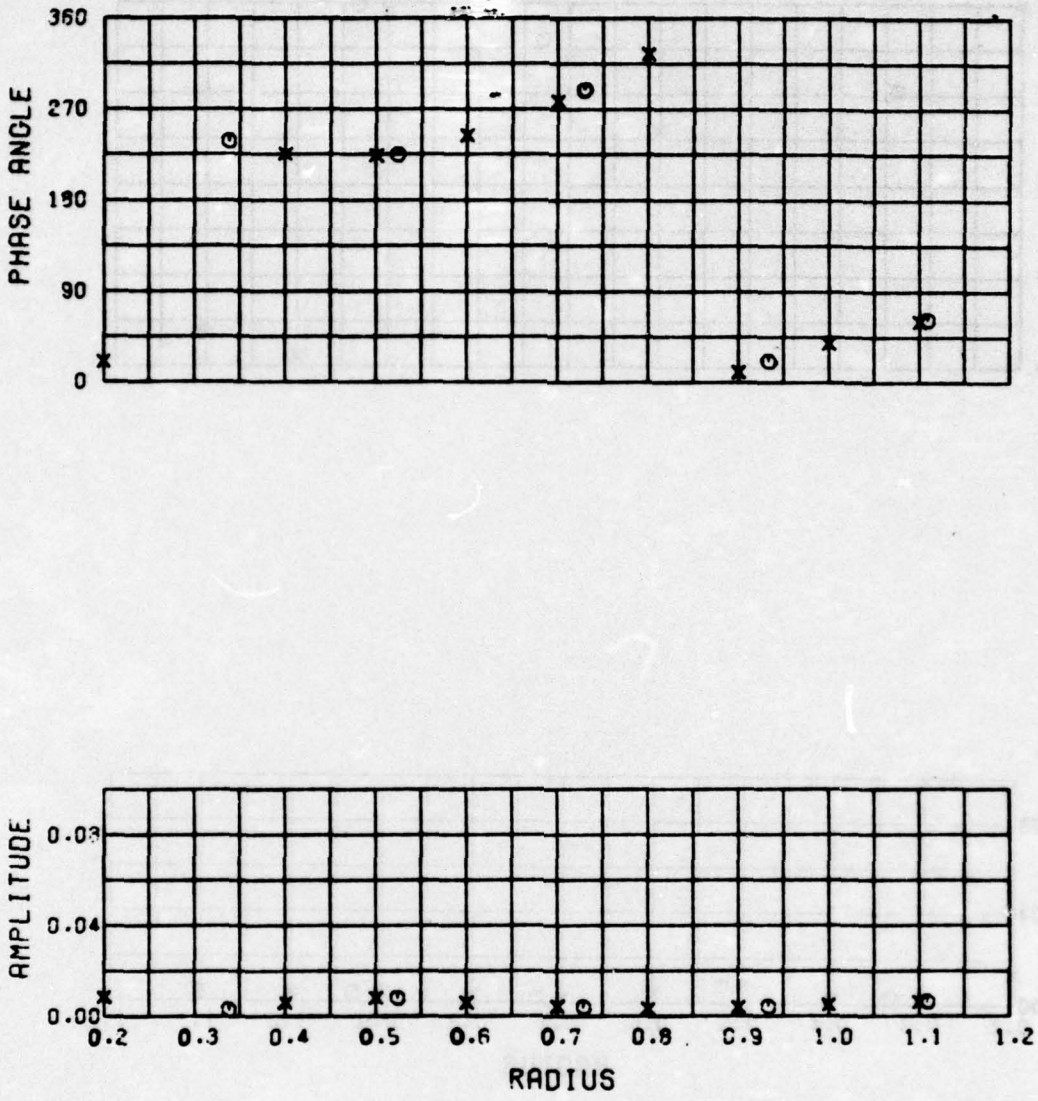

Figure 18 - Radial Distribution of the Amplitude and Phase Angle of the 8th Harmonic of the Circumferential Distribution of the Longitudinal Velocity Component Ratios

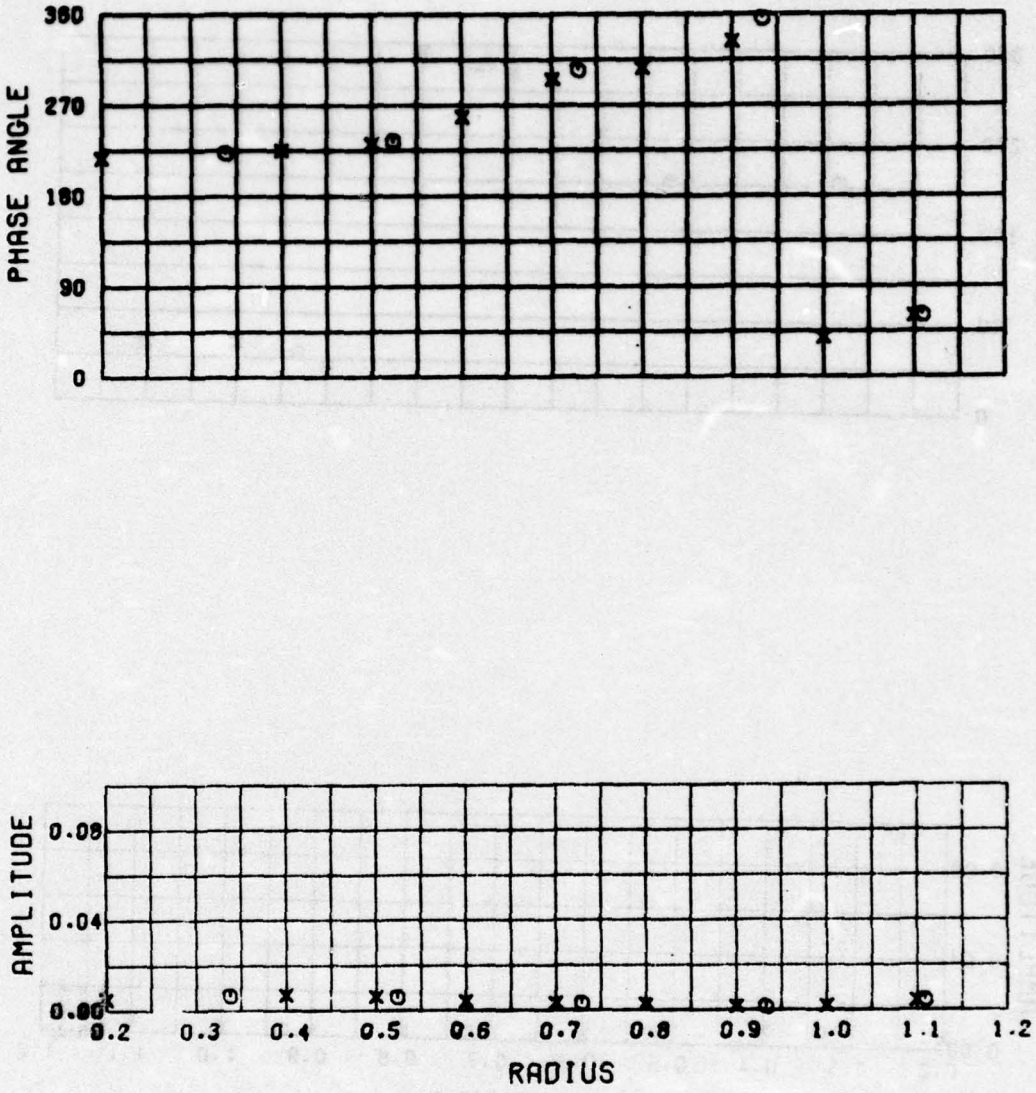

Figure 19 - Radial Distribution of the Amplitude and Phase Angle of the 9th Harmonic of the Circumferential Distribution of the Longitudinal Velocity Component Ratios

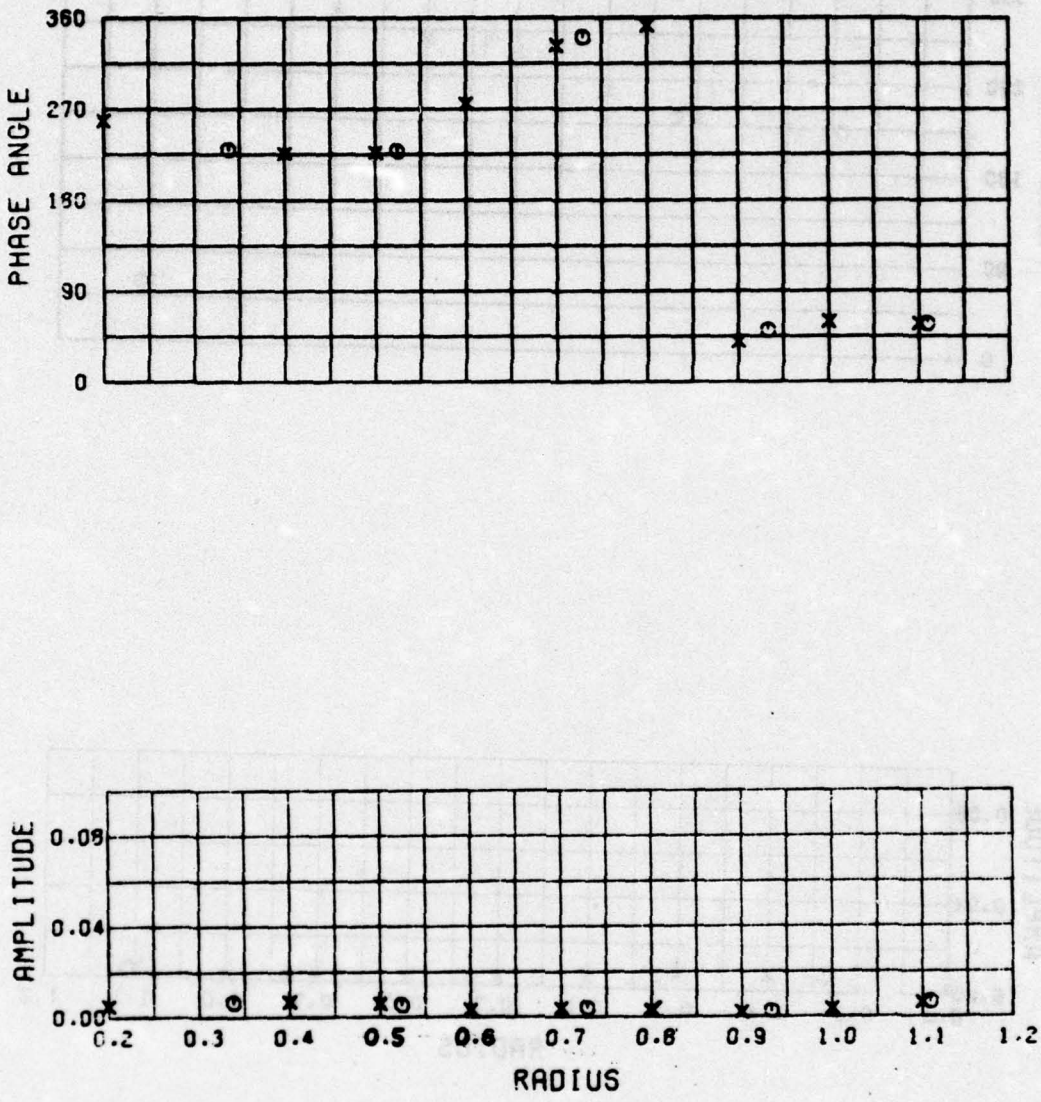

Figure 20 - Radial Distribution of the Amplitude and Phase Angle of the 10th Harmonic of the Circumferential Distribution of the Longitudinal Velocity Component Ratio

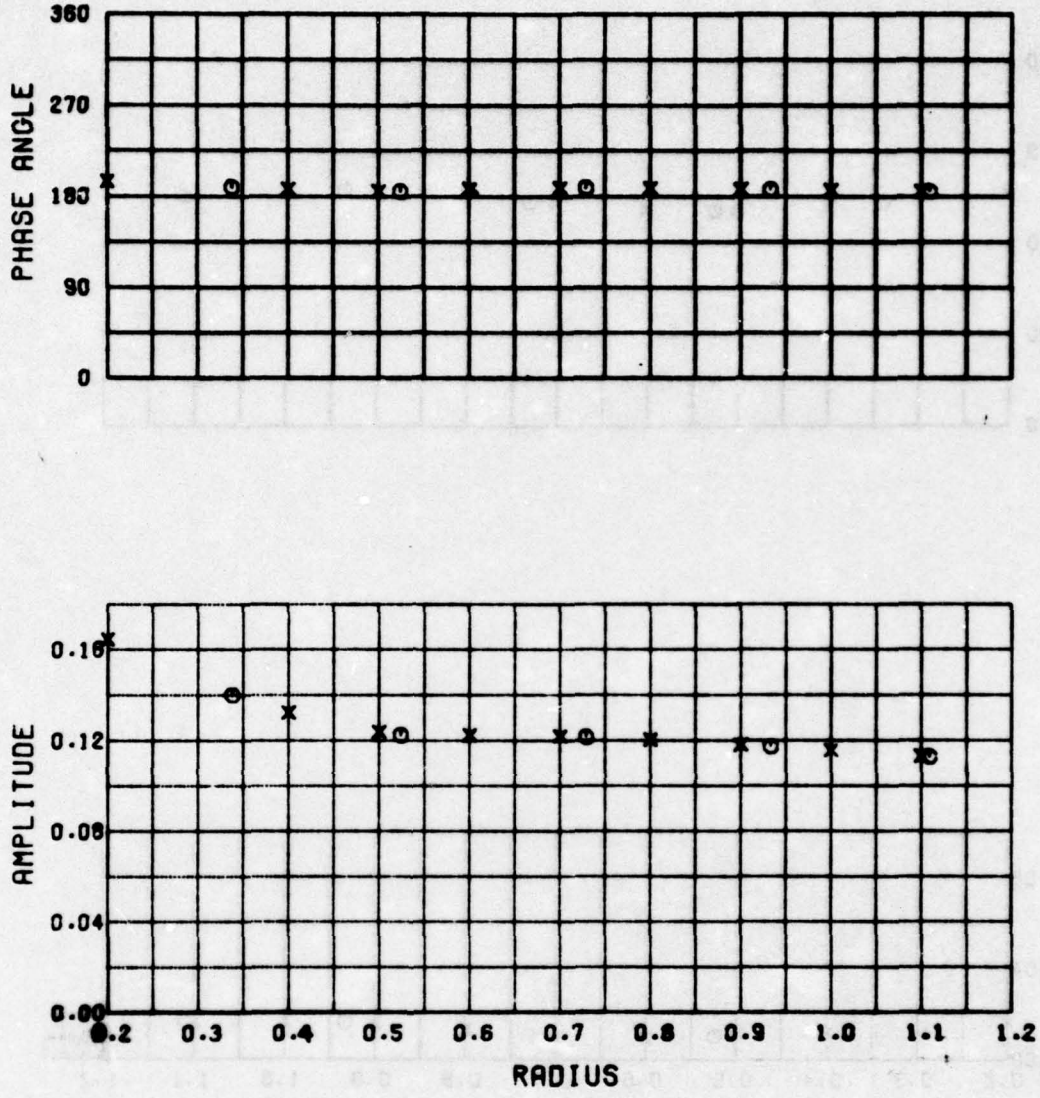

Figure 21 - Radial Distribution of the Amplitude and Phase Angle of the 1st Harmonic of the Circumferential Distribution of the Tangential Velocity Component Ratios

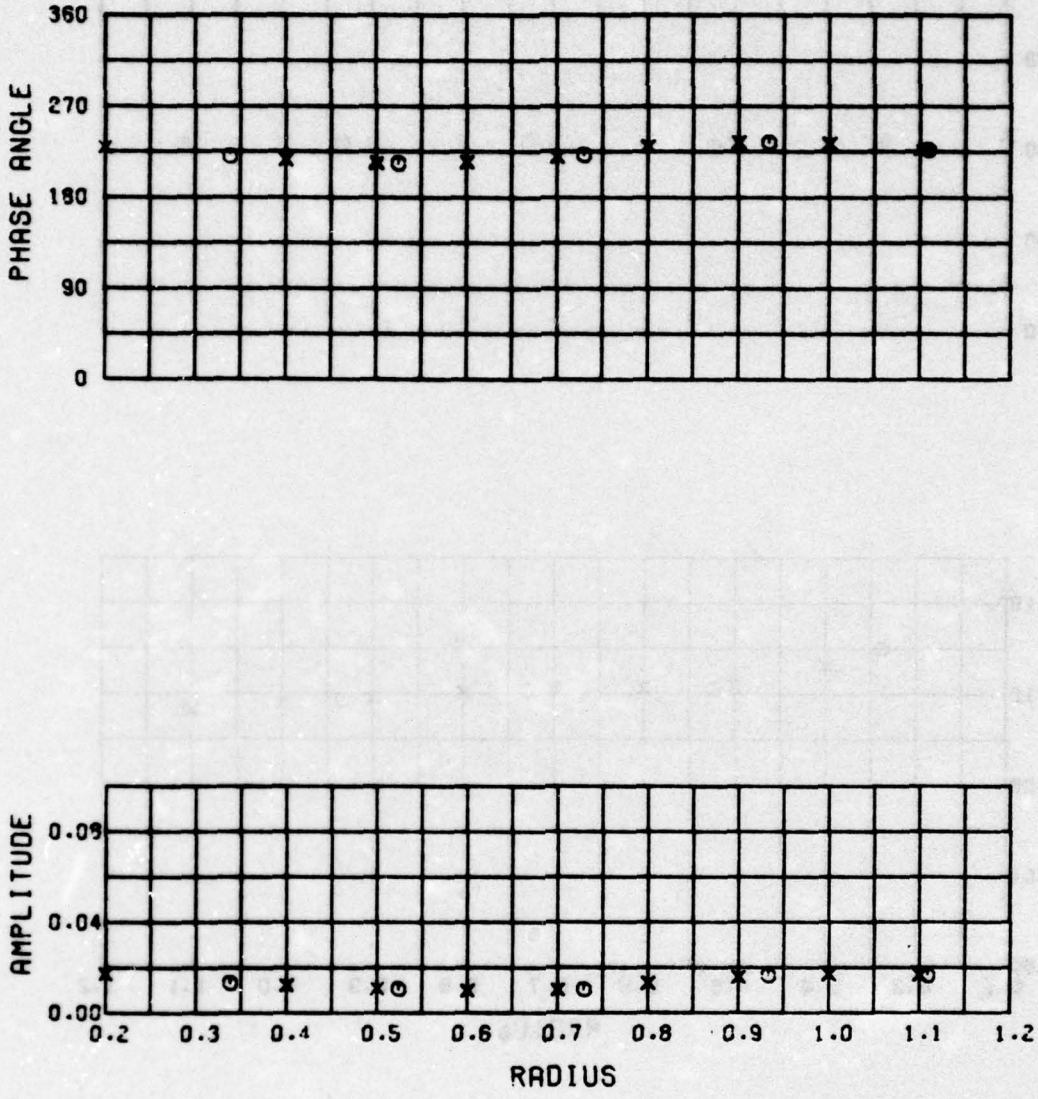

Figure 22 - Radial Distribution of the Amplitude and Phase Angle of the 2nd Harmonic of the Circumferential Distribution of the Tangential Velocity Component Ratios

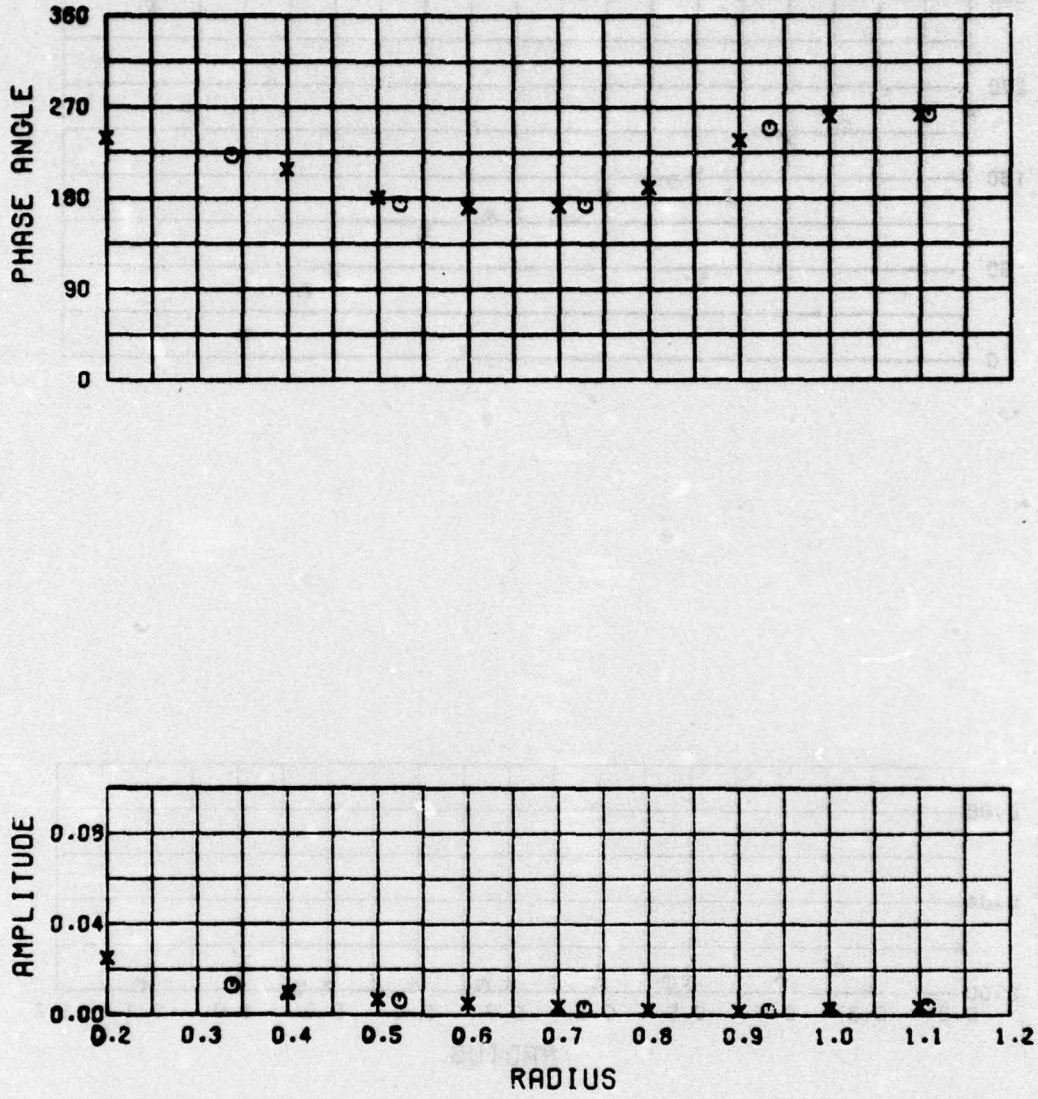

Figure 23 - Radial Distribution of the Amplitude and Phase Angle of the 3rd Harmonic of the Circumferential Distribution of the Tangential Velocity Component Ratios

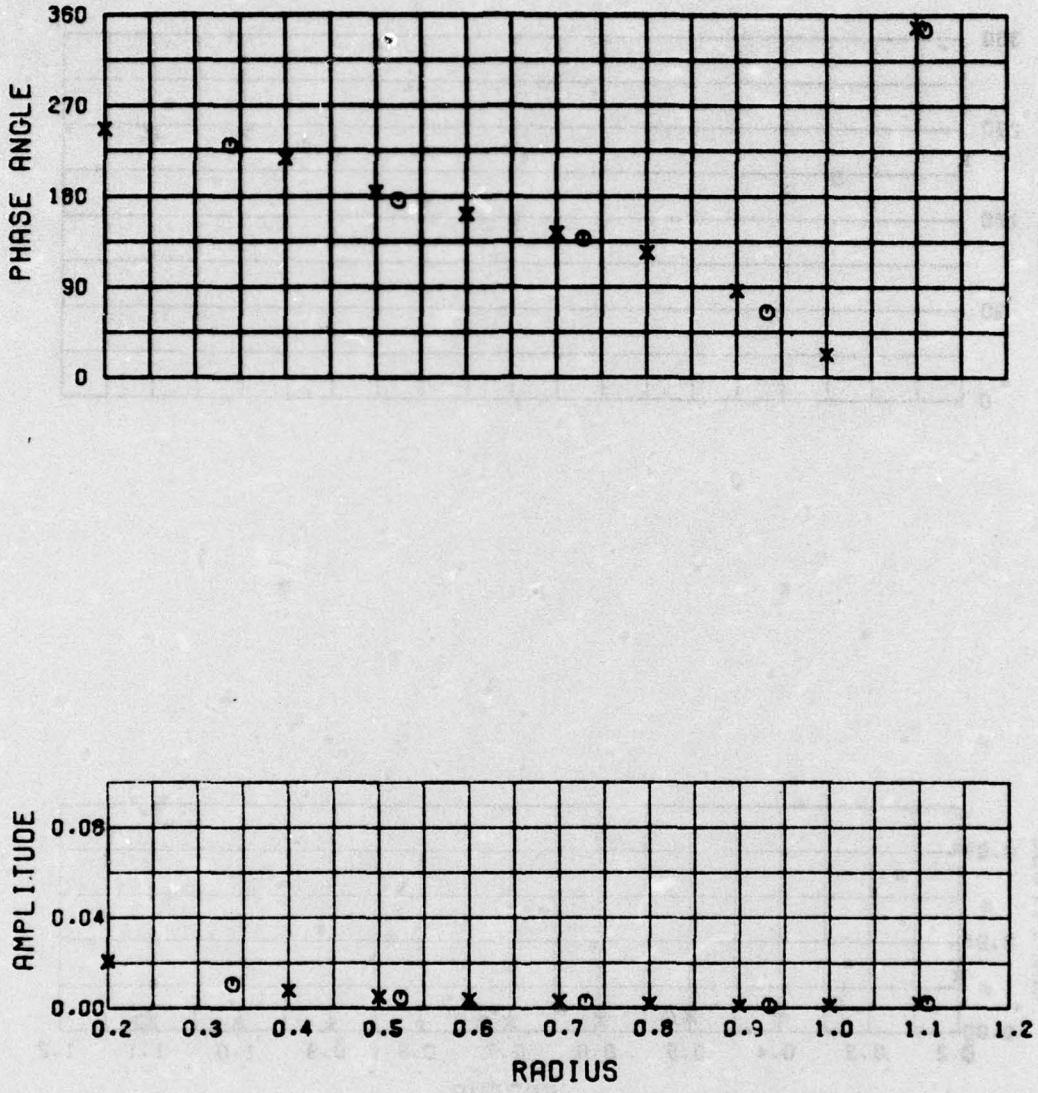

Figure 24 - Radial Distribution of the Amplitude and Phase Angle of the 4th Harmonic of the Circumferential Distribution of the Tangential Velocity Component Ratios

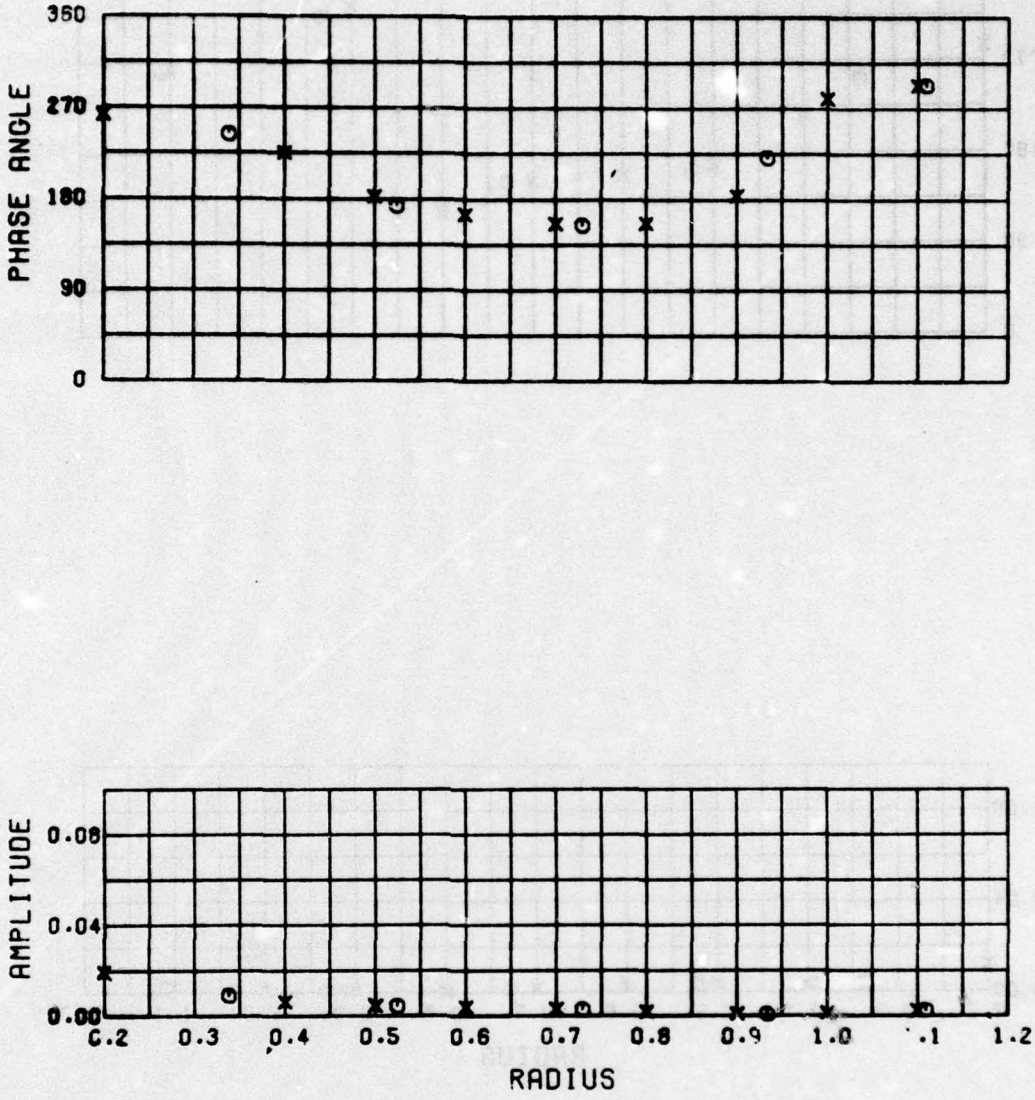

Figure 25 - Radial Distribution of the Amplitude and Phase Angle of the 5th Harmonic of the Circumferential Distribution of the Tangential Velocity Component Ratios

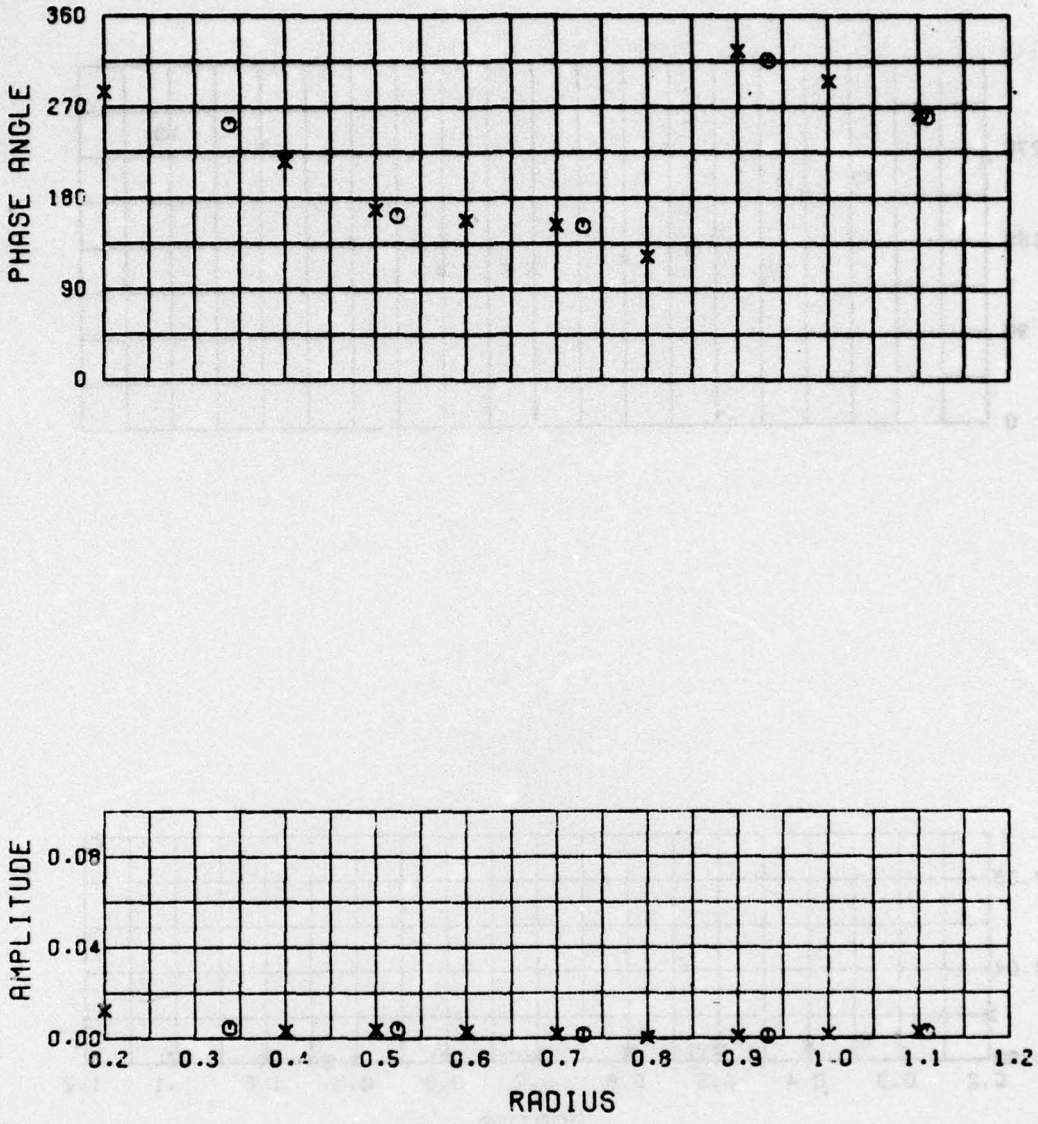

Figure 26 - Radial Distribution of the Amplitude and Phase Angle of the 6th Harmonic of the Circumferential Distribution of the Tangential Velocity Component Ratios

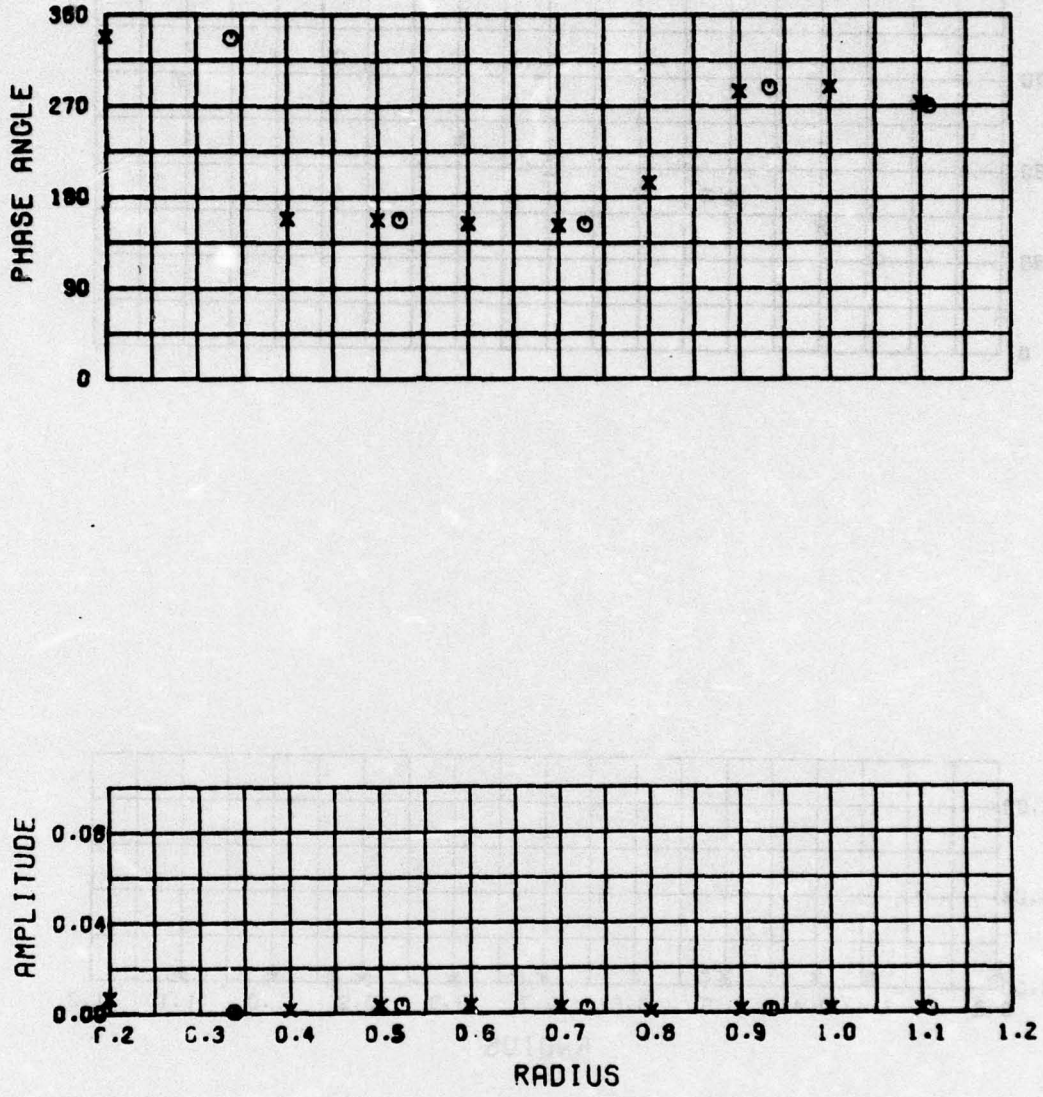

Figure 27 - Radial Distribution of the Amplitude and Phase Angle of the 7th Harmonic of the Circumferential Distribution of the Tangential Velocity Component Ratios

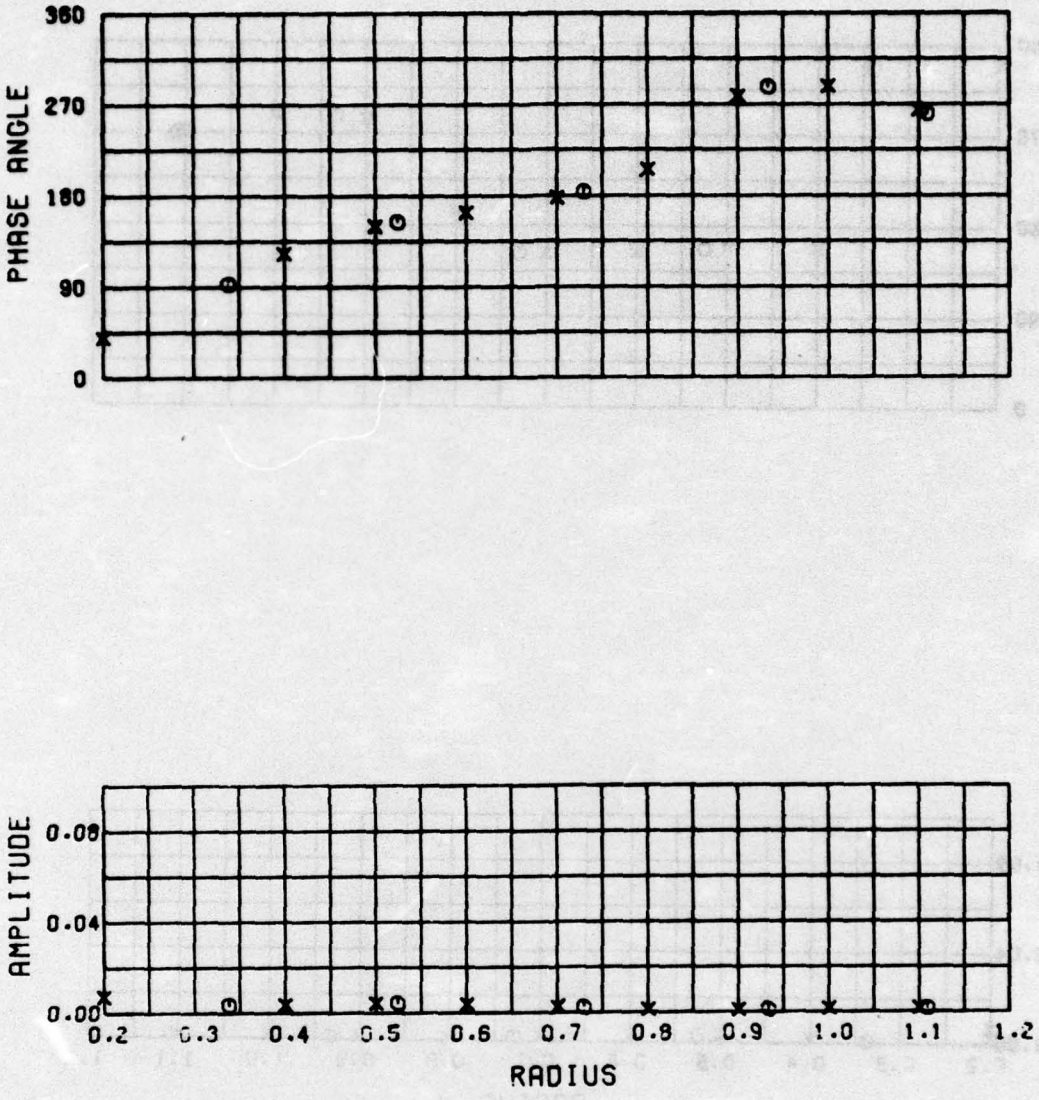

Figure 28 - Radial Distribution of the Amplitude and Phase Angle of the 8th Harmonic of the Circumferential Distribution of the Tangential Velocity Component Ratios

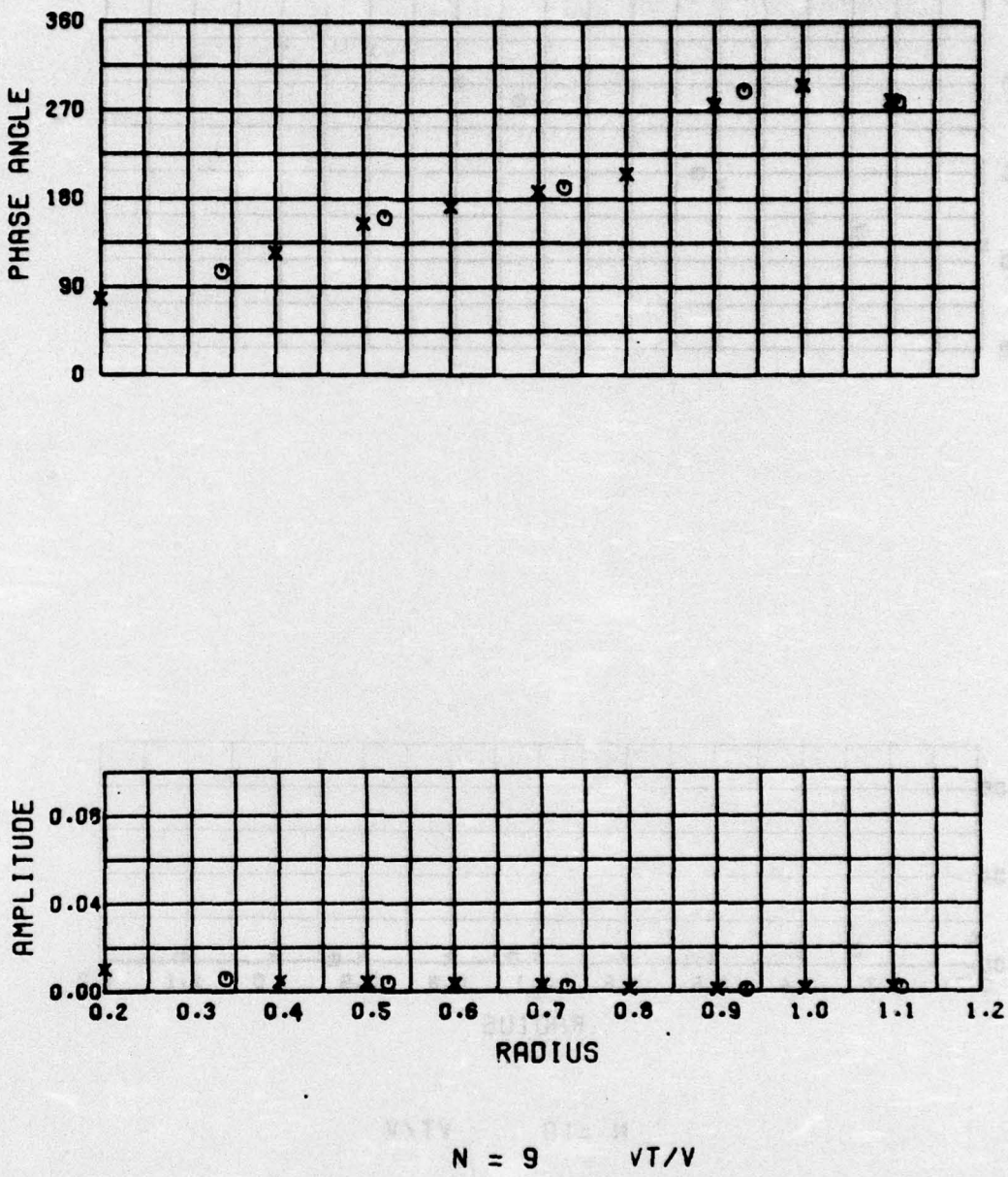

Figure 29 - Radial Distribution of the Amplitude and Phase Angle of the 9th Harmonic of the Circumferential Distribution of the Tangential Velocity Component Ratios

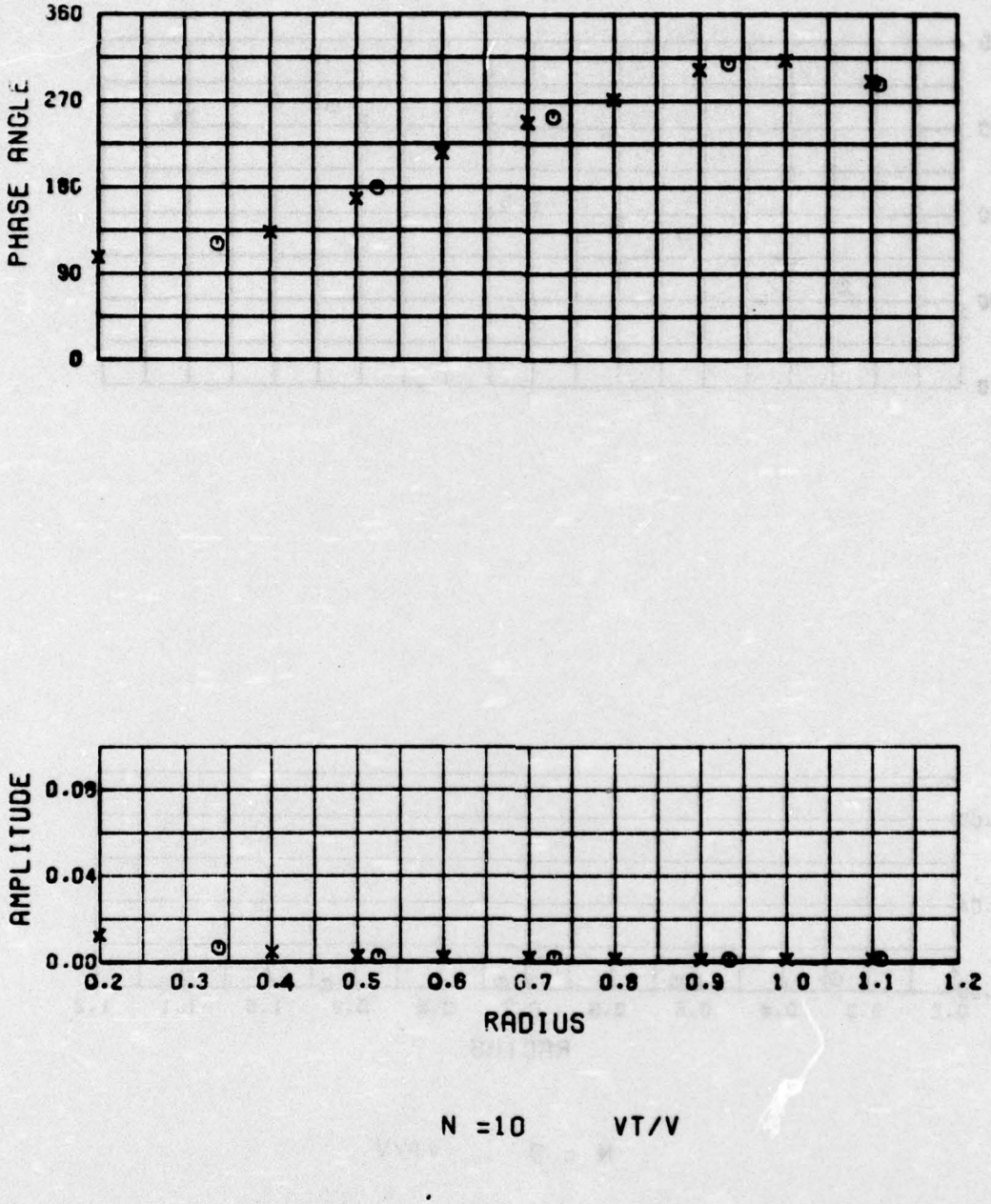

Figure 30 - Radial Distribution of the Amplitude and Phase Angle of the 10th Harmonic of the Circumferential Distribution of the Tangential Velocity Component Ratios

Table 1 - Listing of the Mean Velocity Component Ratios, the Mean Advance Angles and other Derived Quantities at the Experimental and the Interpolated Radii

PROPELLER DIAMETER = 18.00 FEET JA = 1.051

RADIUS =	.339	.524	.729	.933	1.109	.200	.400	.500	.600	.700	.800	.900	1.000	1.100
VXBAR =	.946	.945	.929	.911	.899	.938	.947	.946	.940	.932	.923	.914	.906	.899
VTBAR =	-.016	-.010	-.004	.010	-.015	-.021	-.014	-.010	-.008	-.005	.006	.011	.004	-.013
VRBAR =	.090	.062	.073	.043	.066	.133	.077	.064	.071	.074	.055	.044	.046	.063
1-WVX =	.943	.945	.941	.933	.924	0.000	.944	.946	.945	.942	.939	.934	.929	.925
1-WX =	.987	.969	.956	.941	.930	0.000	.981	.972	.965	.958	.951	.943	.936	.930
BBAR =	43.57	31.27	23.14	18.03	15.24	58.41	38.71	32.52	27.77	24.06	21.05	18.69	16.84	15.35
BPOS =	4.99	2.79	2.08	1.72	1.22	10.17	3.98	2.96	2.42	2.14	2.01	1.81	1.52	1.24
THETA =	70.00	77.50	67.50	67.50	77.50	7.50	70.00	77.50	67.50	67.50	65.00	67.50	70.00	75.00
BNEG =	-6.23	-3.68	-3.93	-3.08	-3.89	-14.84	-5.03	-3.93	-3.44	-3.89	-3.63	-3.21	-3.14	-3.80
THETA =	327.50	322.50	317.50	317.50	342.50	327.50	322.50	322.50	320.00	317.50	317.50	317.50	347.50	345.00

VXBAR IS CIRCUMFERENTIAL MEAN LONGITUDINAL VELOCITY.
VTBAR IS CIRCUMFERENTIAL MEAN TANGENTIAL VELOCITY.
VRBAR IS CIRCUMFERENTIAL MEAN RADIAL VELOCITY.
1-WVX IS VOLUMETRIC MEAN WAKE VELOCITY WITHOUT TANGENTIAL CORRECTION.
1-WX IS VOLUMETRIC MEAN WAKE VELOCITY WITH TANGENTIAL CORRECTION.
BBAR IS MEAN ANGLE OF ADVANCE.
BPOS IS VARIATION BETWEEN THE MAXIMUM AND MEAN ADVANCE ANGLES (DELTA BETA PLUS).
BNEG IS VARIATION BETWEEN THE MINIMUM AND MEAN ADVANCE ANGLES (DELTA BETA MINUS).
THETA IS ANGLE IN DEGREES AT WHICH CORRESPONDING BPOS OR BNEG OCCURS.

Table 2 - Harmonic Analyses of Longitudinal Velocity Component Ratios at the Experimental Radii

PROPELLER DIAMETER = 18.00 FEET JA = 1.051

HARMONIC ANALYSES OF LONGITUDINAL VELOCITY COMPONENT RATIOS (VX/V)

HARMONIC =	1	2	3	4	5	6	7	8	9	10
RADIUS = .338										
AMPLITUDE =	.0461	.0445	.0367	.0205	.0147	.0073	.0036	.0030	.0067	.0065
PHASE ANGLE =	278.2	295.9	298.4	318.7	311.7	343.3	274.4	238.3	222.5	229.9
RADIUS = .524										
AMPLITUDE =	.0234	.0233	.0179	.0039	.0077	.0064	.0079	.0081	.0059	.0054
PHASE ANGLE =	295.8	294.2	285.7	298.4	236.2	226.2	217.8	225.0	234.1	228.5
RADIUS = .729										
AMPLITUDE =	.0459	.0283	.0185	.0054	.0019	.0011	.0024	.0039	.0032	.0040
PHASE ANGLE =	296.3	293.7	305.6	311.7	299.4	345.2	323.2	289.4	304.9	340.6
RADIUS = .933										
AMPLITUDE =	.0495	.0425	.0268	.0035	.0035	.0048	.0039	.0041	.0013	.0024
PHASE ANGLE =	278.5	288.2	286.0	341.5	100.0	71.1	357.1	20.6	355.6	50.8
RADIUS = 1.109										
AMPLITUDE =	.0934	.0534	.0342	.0093	.0078	.0061	.0054	.0063	.0045	.0065
PHASE ANGLE =	272.6	278.0	285.2	326.9	1.3	29.5	32.6	62.2	61.2	57.5

Table 3 - Harmonic Analyses of Longitudinal Velocity Component Ratios at the Interpolated Radii

PROPELLER DIAMETER = 18.00 FEET JA = 1.051

HARMONIC ANALYSES OF LONGITUDINAL VELOCITY COMPONENT RATIOS (VX/V)

HARMONIC =	1	2	3	4	5	6	7	8	9	10
RADIUS = .200										
AMPLITUDE =	.0905	.0759	.0640	.0443	.0350	.0258	.0137	.0085	.0051	.0049
PHASE ANGLE =	274.7	296.5	306.3	321.5	335.5	8.2	359.7	20.8	216.8	258.4
RADIUS = .400										
AMPLITUDE =	.0337	.0347	.0283	.0130	.0099	.0039	.0056	.0058	.0068	.0067
PHASE ANGLE =	282.3	295.5	293.7	315.7	288.2	292.4	233.8	225.5	225.3	226.2
RADIUS = .500										
AMPLITUDE =	.0239	.0247	.0193	.0050	.0078	.0060	.0079	.0081	.0062	.0058
PHASE ANGLE =	293.2	294.5	286.6	303.8	243.6	230.5	218.6	224.1	231.8	226.9
RADIUS = .600										
AMPLITUDE =	.0342	.0241	.0170	.0049	.0049	.0036	.0042	.0059	.0041	.0031
PHASE ANGLE =	299.1	295.1	298.6	304.0	251.6	239.1	233.2	243.8	258.4	275.8
RADIUS = .700										
AMPLITUDE =	.0440	.0270	.0179	.0054	.0024	.0011	.0021	.0042	.0032	.0037
PHASE ANGLE =	297.5	294.3	305.8	309.8	284.5	300.8	302.7	277.8	295.9	332.3
RADIUS = .800										
AMPLITUDE =	.0412	.0336	.0211	.0035	.0016	.0023	.0031	.0032	.0025	.0025
PHASE ANGLE =	290.8	292.9	295.2	323.4	129.3	71.5	335.0	324.7	306.6	352.1
RADIUS = .900										
AMPLITUDE =	.0453	.0404	.0254	.0031	.0035	.0044	.0038	.0037	.0015	.0020
PHASE ANGLE =	281.1	289.6	287.3	340.8	109.9	74.3	351.2	9.8	333.2	39.4
RADIUS = 1.000										
AMPLITUDE =	.0619	.0467	.0297	.0049	.0034	.0053	.0044	.0049	.0019	.0036
PHASE ANGLE =	274.8	284.7	284.6	337.0	63.0	60.2	10.0	38.5	38.8	59.7
RADIUS = 1.100										
AMPLITUDE =	.0903	.0529	.0338	.0088	.0072	.0060	.0053	.0062	.0042	.0062
PHASE ANGLE =	272.6	278.6	285.0	327.6	4.1	32.5	30.8	60.4	60.4	57.9

Table 4 - Harmonic Analyses of Tangential Velocity Component Ratios at the Experimental Radii

PROPELLER DIAMETER = 18.00 FEET JA = 1.051

HARMONIC ANALYSES OF TANGENTIAL VELOCITY COMPONENT RATIOS (VT/V)

HARMONIC =	1	2	3	4	5	6	7	8	9	10
RADIUS = .338										
AMPLITUDE =	.1399	.0134	.0130	.0107	.0090	.0045	.0005	.0035	.0057	.0067
PHASE ANGLE =	188.9	220.3	221.9	230.4	243.6	252.4	336.9	93.1	105.5	121.1
RADIUS = .524										
AMPLITUDE =	.1224	.0106	.0062	.0047	.0043	.0039	.0035	.0042	.0040	.0025
PHASE ANGLE =	184.8	213.4	174.2	175.5	173.2	162.7	157.6	153.9	160.3	179.4
RADIUS = .729										
AMPLITUDE =	.1215	.0104	.0033	.0027	.0027	.0015	.0022	.0022	.0024	.0024
PHASE ANGLE =	188.3	221.7	173.6	137.9	154.6	152.3	153.2	182.9	192.0	253.3
RADIUS = .933										
AMPLITUDE =	.1172	.0165	.0020	.0010	.0005	.0011	.0016	.0010	.0009	.0012
PHASE ANGLE =	186.5	234.2	249.3	64.8	221.4	315.8	288.7	286.8	290.4	308.7
RADIUS = 1.109										
AMPLITUDE =	.1127	.0166	.0039	.0021	.0024	.0026	.0015	.0016	.0018	.0013
PHASE ANGLE =	184.7	227.0	262.4	345.9	293.1	260.3	269.7	261.0	278.2	287.7

Table 5 - Harmonic Analyses of Tangential Velocity Component Ratios at the Interpolated Radii

PROPELLER DIAMETER = 18.00 FEET JA = 1.051

HARMONIC ANALYSES OF TANGENTIAL VELOCITY COMPONENT RATIOS (VT/V)

HARMONIC =	1	2	3	4	5	6	7	8	9	10
RADIUS = .200										
AMPLITUDE =	.1644	.0174	.0250	.0209	.0195	.0124	.0067	.0072	.0103	.0127
PHASE ANGLE =	194.4	228.8	239.1	246.7	262.5	284.8	338.3	39.6	77.6	106.7
RADIUS = .400										
AMPLITUDE =	.1322	.0122	.0096	.0077	.0061	.0032	.0014	.0035	.0046	.0047
PHASE ANGLE =	186.9	216.9	208.6	216.9	225.3	215.4	158.5	123.0	124.3	133.1
RADIUS = .500										
AMPLITUDE =	.1238	.0108	.0066	.0050	.0044	.0038	.0033	.0041	.0040	.0028
PHASE ANGLE =	185.0	213.6	180.6	184.1	182.2	168.2	157.8	150.0	154.4	168.1
RADIUS = .600										
AMPLITUDE =	.1224	.0099	.0051	.0038	.0038	.0030	.0033	.0035	.0034	.0022
PHASE ANGLE =	186.7	214.7	171.4	162.3	164.6	158.4	153.4	163.3	172.1	215.0
RADIUS = .700										
AMPLITUDE =	.1218	.0101	.0037	.0029	.0030	.0019	.0025	.0025	.0027	.0024
PHASE ANGLE =	188.1	219.7	171.8	143.6	156.2	153.4	152.2	177.7	187.3	247.1
RADIUS = .800										
AMPLITUDE =	.1202	.0132	.0022	.0019	.0018	.0003	.0007	.0011	.0012	.0016
PHASE ANGLE =	187.7	230.3	190.8	124.2	156.5	122.4	194.2	205.5	205.3	271.4
RADIUS = .900										
AMPLITUDE =	.1180	.0159	.0018	.0011	.0007	.0009	.0013	.0009	.0007	.0012
PHASE ANGLE =	186.8	234.1	237.6	85.9	183.8	325.1	284.6	278.1	275.8	302.2
RADIUS = 1.000										
AMPLITUDE =	.1156	.0171	.0027	.0012	.0010	.0016	.0018	.0013	.0013	.0012
PHASE ANGLE =	185.8	233.0	261.0	22.1	280.0	295.6	289.1	287.7	296.1	311.8
RADIUS = 1.100										
AMPLITUDE =	.1130	.0167	.0038	.0020	.0022	.0025	.0015	.0015	.0018	.0012
PHASE ANGLE =	184.8	227.7	262.7	347.8	292.9	263.0	272.9	264.2	280.4	290.8

DTNSRDC ISSUES THREE TYPES OF REPORTS

(1) DTNSRDC REPORTS, A FORMAL SERIES PUBLISHING INFORMATION OF PERMANENT TECHNICAL VALUE, DESIGNATED BY A SERIAL REPORT NUMBER.

(2) DEPARTMENTAL REPORTS, A SEMIFORMAL SERIES, RECORDING INFORMATION OF A PRELIMINARY OR TEMPORARY NATURE, OR OF LIMITED INTEREST OR SIGNIFICANCE, CARRYING A DEPARTMENTAL ALPHANUMERIC IDENTIFICATION.

(3) TECHNICAL MEMORANDA, AN INFORMAL SERIES, USUALLY INTERNAL WORKING PAPERS OR DIRECT REPORTS TO SPONSORS, NUMBERED AS TM SERIES REPORTS; NOT FOR GENERAL DISTRIBUTION.